# Analysis of long term drought severity characteristics and trends across semiarid Botswana using two drought indices

Jimmy Byakatonda[a,c,*], B.P. Parida[a], D.B. Moalafhi[b], Piet K. Kenabatho[b]

[a] Department of Civil Engineering, P/Bag UB 0061, University of Botswana, Gaborone, Botswana
[b] Department of Environmental Science, P/Bag UB 00704, University of Botswana, Gaborone, Botswana
[c] Department of Biosystems Engineering, Gulu University, P.O. Box 166, Gulu, Uganda

## ARTICLE INFO

## ABSTRACT

Semiarid areas exhibit high climate variability whose frequency has increased in the recent past. This variability ultimately influences the spatial and temporal characteristics of droughts which in turn require a reliable drought index that can adequately characterize drought both in time and space. This study applied two drought indices viz.: Standardized precipitation index (SPI) and Standardized precipitation and evapotranspiration index (SPEI) at timescales of 1-, 3-, 6-, 12-, 18- and 24-months for a period of 1960–2016. The monotonic changes in drought severity were studied using Mann-Kendall *Z*-statistic and Sen's slope estimator. Both drought indices were able to detect the historical drought events of 1961/62–1965/66, 1980/81–1986/87, 1991/92, 2001/02–2005/06, 2009/10–2012/13 and 2014/15–2015/16. These events mainly coincided with El Niño years, hence the influence of El Niño southern oscillation (ENSO) on drought occurrence could not be ruled out. The drought evolutions were characterized by low frequency and longer durations at timescales of 12-, 18-, and 24-months. It was also observed that SPI overestimated drought severity during dry winter months while SPEI showed higher spatial coverage of drought vulnerability compared to SPI. Spatial and temporal trends of droughts showed significant wetting trends during the period 1960–1979 while during the entire period it was mostly drying tendencies after 1979/80. Pandamatenga and Shakawe showed higher vulnerability towards drying conditions during the period of analysis. The association between SPI and *SPE*I was also investigated using Spearman's rank correlation. Results from this analysis indicate that SPI accounts for > 50% of the variations in SPEI and the association was strongest (96%) at 12-months timescale. The influence of temperature on drought evolutions was demonstrated at Francistown with SPI recording positive trends and SPEI negative ones. This study concludes that with the ongoing global warming, SPEI proves more robust in characterizing droughts in semiarid areas. It is hoped that findings from this study will augment ongoing efforts of mitigating negative impacts of increased incidences of climate variability especially in areas of agriculture and water resource management.

## 1. Introduction

The advent of global warming and increased incidences of climate variability have made understanding of drought evolution more complex and yet drought severity has increased both in magnitude and duration in the recent past (Cook et al., 2014; Dai, 2011; Huang et al., 2016). Droughts manifests differently from other natural hazards such as floods (Heim Jr., 2002; Homdee et al., 2016; Van Loon and Laaha, 2015) in that their onset and cessation is not clearly defined. Droughts manifest in different forms at various time intervals. Drought initially occurs as a result of below normal rainfall for extended periods often referred to as meteorological drought (Sheffield et al., 2012; Van Loon, 2013; Vicente-Serrano et al., 2012). Continued below normal rainfall conditions will have drought progressing into agricultural, hydrological and later into social economical drought (IPCC, 2012; Masud et al., 2015; Wilhite, 2000). For this reason it is important to investigate drought severity at various timescales, sometimes over the year, to understand drought effects on various components of the hydrological cycle. However with the current global temperature rise, there has been a reported increase in evaporative demand further exerting pressure on water and agricultural resources (Vicente-Serrano et al., 2014; Wang et al., 2012). Nevertheless, it is not yet clear if indeed temperature rise automatically translates into increased evaporative demand since one school of thought argues that other meteorological variables such as

wind, relative humidity and sunshine hours may not have varied to the same degree as temperature (McEvoy et al., 2012; Roderick et al., 2007; Vicente-Serrano et al., 2014). It thus becomes necessary to use more than one avenues of quantifying droughts to identify the most appropriate for a particular location of interest.

Due to the complexity of droughts, it is even more difficult to quantify them. The absence of direct methods to measure drought has prompted the use of drought indices which are proxies of drought impacts on hydrological systems (Sheffield et al., 2012; Shukla et al., 2011; Svoboda et al., 2016). Over time a number of drought indices have been developed and used in different parts of the globe to characterize droughts and their propagation in different compartments of the hydrological cycle. Some of the drought indices currently used are the Palmer drought severity index (PDSI) (Palmer, 1965), Drought severity index (DSI) (PaiMazumder et al., 2013), Standardized precipitation index (SPI) (McKee et al., 1993) and more recently Standardized precipitation and evapotranspiration index (SPEI) (Vicente-Serrano et al., 2010) for characterizing climatic droughts. Soil moisture index (SSI) (Golian et al., 2015) and standardized stream flow index (SFI) (Byakatonda et al., 2018; Nalbantis and Tsakiris, 2009) have also been used to study drought propagation in the soil profile and overland flow respectively. In spite of these numerous drought indices, there are no clear guidelines on the most suitable drought index. However, the World Meteorological Organization (WMO) recommends that the choice of a particular index should depend on the availability of data and ease to apply (Masud et al., 2015; Svoboda et al., 2016). This study proposes to investigate the ability of SPI and SPEI to detect and characterize climatic droughts in Botswana. The choice was premised on the need to establish if indeed global warming has had an impact on drought characteristics across the study area due to its location in a semiarid region. Both these indices are multiscalar, only that SPI is precipitation dependent whereas SPEI incorporates both precipitation and evaporation. With the undeniable effects of climate change across the globe, it has become increasingly necessary to study the temporal and spatial variability of drought severity globally as a result of changing climate. This is even more vital in semiarid regions such as Botswana with endemic water shortages (GOB-MMEWR, 2006; Statistics Botswana, 2009). This intervention could help to improve drought preparedness and mitigation measures towards minimizing impacts of global warming in Botswana. The close interaction of drought and the hydrological cycle makes it imperative to generate knowledge on changing patterns of drought severity for sustainable water resources management (Das et al., 2016; He et al., 2015; Oguntunde et al., 2014).

Several studies have been conducted across the world in recent times to investigate drought characteristics and their trends. Das et al. (2016) investigated trends in drought severity using Mann-Kendall and Sen's slope estimator across India and reported increasing trends during the Monsoon in the east and central regions. He et al. (2015), while using SPI, were able to characterize droughts in southern China. Their study revealed that the region was more prone to both floods and droughts. Still in China, Liu et al. (2016) also characterized droughts at timescales of 1-, 3-, 6-, 12- and 24-months using SPI and SPEI in the Loess region. They reported weaker trends with SPEI compared to SPI. In Canada, Masud et al. (2015) investigated meteorological droughts using both SPI and SPEI. Through their study, it was concluded that the southern locations were more vulnerable to droughts. Golian et al. (2015) also applied two drought indices (SPI and SSI) to quantify drought severity in Iran. They applied the Mann-Kendall test and found that the northern and central regions of Iran were experiencing increasing trends in droughts. Increasing trends in drought severity in southern Europe were equally investigated by Vicente-Serrano et al. (2014) using various indices including SPI, SPEI and standardized stream flow index (SFI). Their study reported increased evaporative demand as a result of increasing temperature during the study period. In Bolivia, droughts were characterized by decadal variations by Vicente-Serrano et al. (2015). They also applied SPI and SPEI to

characterize these droughts. They reported lower drought severity trends in the Amazon region. Edossa et al. (2014) also studied drought severity in South Africa and found drying tendencies mainly attributed to El Niño southern oscillation (ENSO) influence.

Botswana has been selected as a study area due to its location in a semiarid region with past incidences of more severe and frequent droughts (Byakatonda et al., 2018b). The most severe drought on record is the recent occurrence of 2015/16. This drought caused heavy agricultural losses and water shortages including drying of Gaborone dam which is the main source of water supply to the county's capital. In Botswana although SPI has been applied to study drought characteristics by Batisani (2011), trends in drought severity were not investigated. In another related study, Moalafhi et al. (2017) used SPI as one of the drought indices to assess performance of the Weather Research and Forecasting (WRF) model against mostly global gridded precipitation dataset over the Limpopo river basin. This basin is shared by four southern African member countries including Botswana. In their findings they reported that gridded data exhibited comparable characteristics with observed data. However use of gridded data has its own challenges as it sometimes lacks local attributes in terms of topography and vegetation effects (Usman and Reason, 2004). For this reason, the current study proposes the use of station based meteorological data. It is evident that SPI and SPEI have been extensively used globally but indices developed for one region may not be extrapolated to other regions (Dai, 2013; Heim Jr., 2002; Mishra et al., 2015). It is therefore necessary to adapt and test the ability of specific indices to characterize droughts locally. Besides, it is also necessary to periodically update these indices and detect any changes to facilitate regional water resource planning and management.

Due to the fact that SPI has been widely applied to characterize climatic droughts across southern Africa, Botswana inclusive and with the advent of global warming, it has become imperative to introduce SPEI with an evapotranspiration (ET) component. Hence this study attempts to appraise the ability of these two indices in detecting and characterizing climatic drought. The SPEI retains attributes of PDSI because of the ET component while maintaining the multiscalar nature of SPI (Byakatonda et al., 2016; Svoboda et al., 2016; Vicente-Serrano et al., 2010). The present study therefore intends to investigate drought characteristics and their temporal trends across Botswana at timescales of 1-, 3-, 6-, 12-, 18- and 24-months using SPI and SPEI. The study specific objectives are: (i) To characterize drought severity using SPI and SPEI at timescales of 1-, 3-, 6-, 12-, 18- and 24-months, (ii) Assess trends in drought severity using Mann-Kendall and Sen's slope estimator and (iii) Determine the association between SPI and SPEI across timescales using Spearman's correlation. The varied timescale allows investigation of the behavior of these climatic droughts as they interact with various components of the hydrological cycle. The 1–3-months timescale allows quantification of short term precipitation shortfalls and often referred to as meteorological or climatological drought. 3–6-months timescale accounts for moisture deficit over an agricultural season (Byakatonda et al., 2018c). This drought category is normally referred to as agricultural drought. The 6–12-months timescale depicts seasonal to medium term moisture deficits. It is an aggregation of deficits over an entire season say wet or dry season. Lastly, the 12–24 months timescale provides information on long term droughts which can be linked to river flow, reservoir storage and in some extreme circumstances to ground water storage. It is also often referred to as hydrological drought (Hayes et al., 2011).

## 2. Study area and data

### 2.1. Study area

Botswana, which is located in southern Africa, is situated between 18°S and 27°S often referred to as mid-latitudes. It also stretches between 20°E and 30°E, bordering Namibia, Angola, Zambia, Zimbabwe
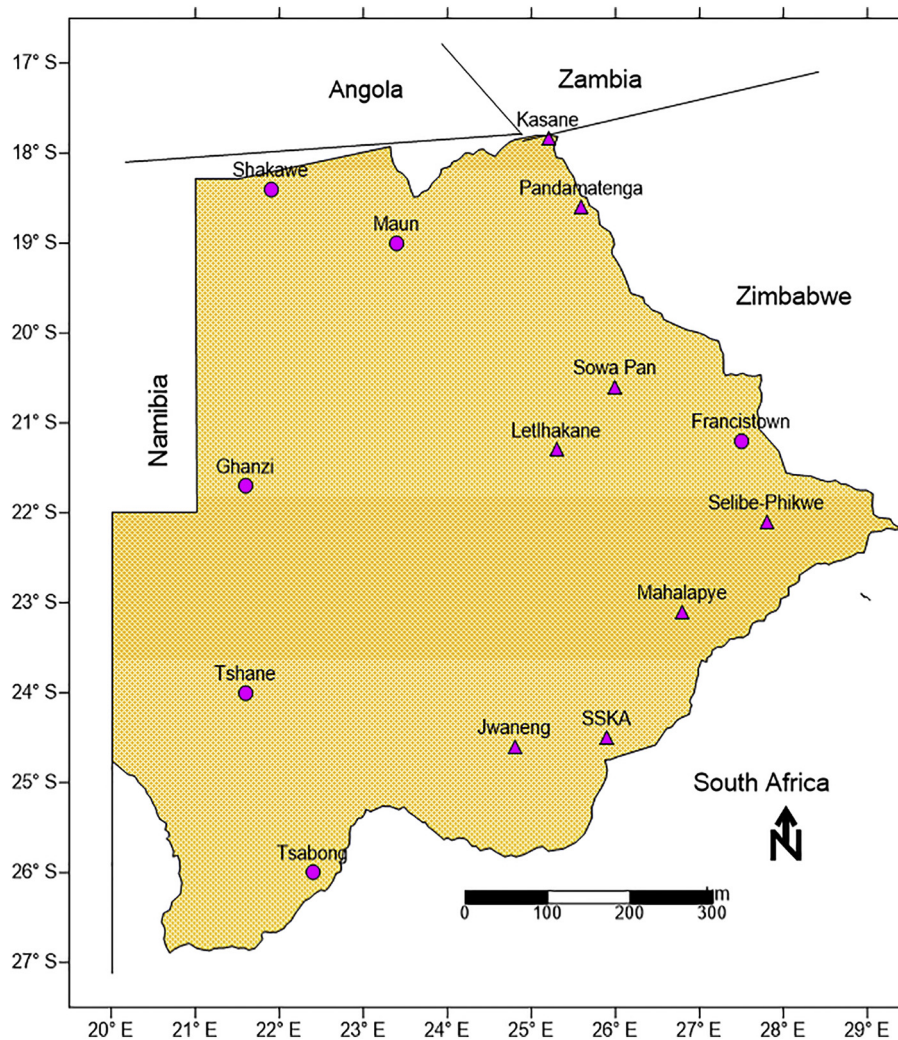
**Fig. 1.** Spatial distribution of meteorological stations across the study area. Stations with round markers are those with climatic dataset starting 1960.

and South Africa (Fig. 1).

Botswana's climate is classified as semiarid with low rainfall and hot summer months (October–April) (Batisani and Yarnal, 2010; Byakatonda et al., 2018b). Rainfall formation is mainly influenced by the shifting of the Inter Tropical Convergence Zone (ITCZ) between November and March for latitudes below 20° S. At higher latitudes, climate is moderated largely by easterlies from the Indian Ocean and westerlies originating from the Atlantic Ocean (Byakatonda et al., 2018b; Nicholson et al., 2001). Rainfall is largely suppressed during El Niño episodes (Byakatonda et al., 2018d). Summer months are characterized by clear skies which facilitates high solar radiation. This coupled with low relative humidity leads to high evaporation rates almost four times higher than the amount of rainfall received (Byakatonda et al., 2016). These conditions then lead to high evaporation rates from open water bodies and soils ultimately affecting both surface water and soil moisture storages. As a result of this, Botswana experiences one of the lowest cereal yields on the African continent (Byakatonda et al., 2018c). A combination of erratic rainfall and high evaporative demand has made droughts a common occurrence in Botswana. Current disaster records indicate that from 1960 to date, droughts have become more frequent and severe. The drought years on record are 1961–1965, 1979/80, 1981–1987, 1991–1999, 2001–2005, 2009–2013 and the most recent of 2014–2016 (Statistics Botswana, 2016). The drought events that occurred during the overlapping period of 2000–2016 for all the stations are shown on Fig. 2. The plot in Fig. 2 shows that during periods of low rainfall, temperature peaks were

recorded. This probably indicates an inverse relationship between rainfall and temperature across the study area.

### 2.2. Climatic dataset

Climatic data was provided by the Department of Meteorological Services (DMS) of Botswana. The data comprised of monthly rainfall, maximum and minimum temperature from 14 synoptic stations spread across the study area as shown in Fig. 1. The datasets are of varying lengths as presented in Table 1 with the longest being 1960–2016. Of all these stations, six have data records stretching to earlier than 1980.

Earlier studies by Parida and Moalafhi (2008) have reported a decrease in rainfall across the study area from 1979/80. For this foregoing reason, it is necessary to investigate trends in droughts before and after this year. This was possible with the six stations having longer datasets. Hence the periods of trend analysis at these stations were 1960–1979 and the entire period 1960–2016 at all the stations. The homogeneity of the datasets was tested using the standard normal homogeneity (Alexandersson, 1986) and the petit (Pettit, 1979) tests which have been found adequate in various studies involving meteorological time series (Byakatonda et al., 2018d; Hänsel et al., 2016; Wijngaard et al., 2003). However as observed in Table 1 the data length at some synoptic stations is shorter than 30 years to enable effective tracking of the climate change signal as recommended by the World Meteorological Organization (WMO). This does not in any way compromise the findings from this study as a recent and related study by Kumar et al. (2016)
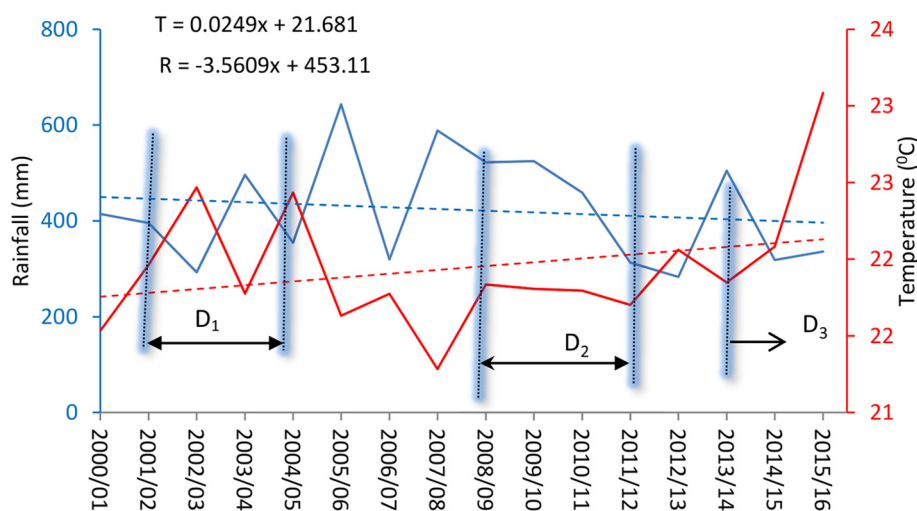
**Fig. 2.** Time series of rainfall (blue line) and temperature (red line) linear trends during the overlapping period (2000–2016) for averages of all synoptic stations showing the recorded drought events of 2001–2005 ($D_1$), 2009–2014 ($D_2$) and 2014–2016 ($D_3$). (For interpretation of the references to colour in this figure legend, the reader is referred to the web version of this article.)

have reported reliable results while using data as short as 10 years. Nevertheless, any climatic trends reported in this study could be more attributed to climate variability rather than change.

A preliminary investigation of linear trends in rainfall and mean temperature at six synoptic stations which are spatially balanced was made and its finding is presented in Fig. 3. The stations selected in this case are Francistown in the east, Ghanzi in the west, Mahalapye located in the south, Maun and Shakawe in the north and Tsabong in the southwest of the study area. These stations are not necessarily those with climatic data starting from 1960 but rather fairly distributed spatially and falling into the respective regions. Linear trends from these stations reveal that temperature has been on the increase in all the regions of the study area. At the same time rainfall has also been experiencing a decreasing trend in all the regions except in the east at Francistown and Ghanzi in the west during the period of study. This corroborates earlier findings by Kenabatho et al. (2012) who observed that temperature rise implicitly reduces rainfall across Botswana. It hence becomes necessary to investigate how these two climatic variables influence drought behavior across the study area.

## 3. Methods

### 3.1. Drought indices

Determination and characterization of drought severity based on Standardized precipitation index (SPI) and Standardized precipitation and evapotranspiration index (SPEI) is presented in this subsection. The

computational steps for SPEI as presented in Edossa et al. (2014) and Byakatonda et al. (2016, 2018d) are summarized as follows;

1. Determination of monthly potential evapotranspiration ($ET_0$). In this study the Hargreaves method is used due to absence of data on wind speed and relative humidity. This method has been found to give comparable results with those of the Penman-Monteith formular when applied to semiarid environments (Byakatonda et al., 2018b, 2018c; Stagge et al., 2014).
2. Computation of the monthly climatic water balance which is the difference between monthly rainfall and $ET_0$ determined in step 1.
3. The climatic water balance is then aggregated at the suggested timescales of 1-, 3-, 6-, 12-, 18- and 24-months.
4. The aggregated water balance in (3) above is then fitted to an appropriate probability density function (pdf) using the probability weighted moments (PWMs) and L-moment technique as described in (Hosking and Wallis, 2005). A number of methods exist for identifying an appropriate distribution that can fit a given climatic dataset. However with small samples and data containing outliers, the method of PWMs and L-moments has been found to produce least bias parameter estimates compared to other methods (Beguería et al., 2014; Byakatonda et al., 2016; Hosking and Wallis, 2005).
5. A cumulative density function (CDF) of the identified pdf is then determined. In this study the generalized logistic (GLO) was found to fit the aggregated climatic water balance series at majority of the stations across timescales.
6. The CDF in (5) above is standardized through a Gaussian

**Table 1**
Rainfall and temperature data record details from meteorological stations used in the study.

| SN | Station Name | Latitude | Longitude | Elevation. | Period of record | | Annual rainfall | |
|----|----|----|----|----|----|----|----|----|
| | | °S | °E | Amsl (m) | Rainfall | Temperature | Totals (mm) | CV (%) |
| 1 | Francistown | 21.2 | 27.5 | 968 | 1960–2016 | 1960–2016 | 485.2 | 37 |
| 2 | Ghanzi | 21.7 | 21.6 | 1131 | 1960–2016 | 1961–2016 | 434.3 | 40 |
| 3 | Jwaneng | 24.6 | 24.8 | 935 | 1988–2016 | 1989–2016 | 450.2 | 30 |
| 4 | Kasane | 17.8 | 25.2 | 960 | 1968–2016 | 1983–2016 | 606.9 | 26 |
| 5 | Letlhakane | 21.3 | 25.3 | 991 | 1993–2016 | 1994–2016 | 396.4 | 37 |
| 6 | Mahalapye | 23.1 | 26.8 | 1005 | 1960–2016 | 1971–2016 | 451.2 | 34 |
| 7 | Maun | 19.0 | 23.4 | 945 | 1960–2016 | 1965–2016 | 454.8 | 39 |
| 8 | Pandamatenga | 17.8 | 28.6 | 1071 | 1998–2016 | 1998–2016 | 517.5 | 30 |
| 9 | Selibe-Phikwe | 23.1 | 37.8 | 892 | 1998–2016 | 2000–2016 | 376.0 | 32 |
| 10 | Shakawe | 18.4 | 21.9 | 1030 | 1960–2016 | 1965–2016 | 522.9 | 35 |
| 11 | SSKA | 24.7 | 25.9 | 975 | 1985–2016 | 1985–2016 | 481.4 | 35 |
| 12 | Sowa Pan | 20.6 | 26.0 | 908 | 1992–2016 | 2000–2016 | 455.2 | 41 |
| 13 | Tsabong | 26.0 | 22.4 | 960 | 1960–2016 | 1961–2016 | 306.5 | 43 |
| 14 | Tshane | 24.0 | 21.6 | 1118 | 1960–2016 | 1961–2016 | 345.1 | 42 |
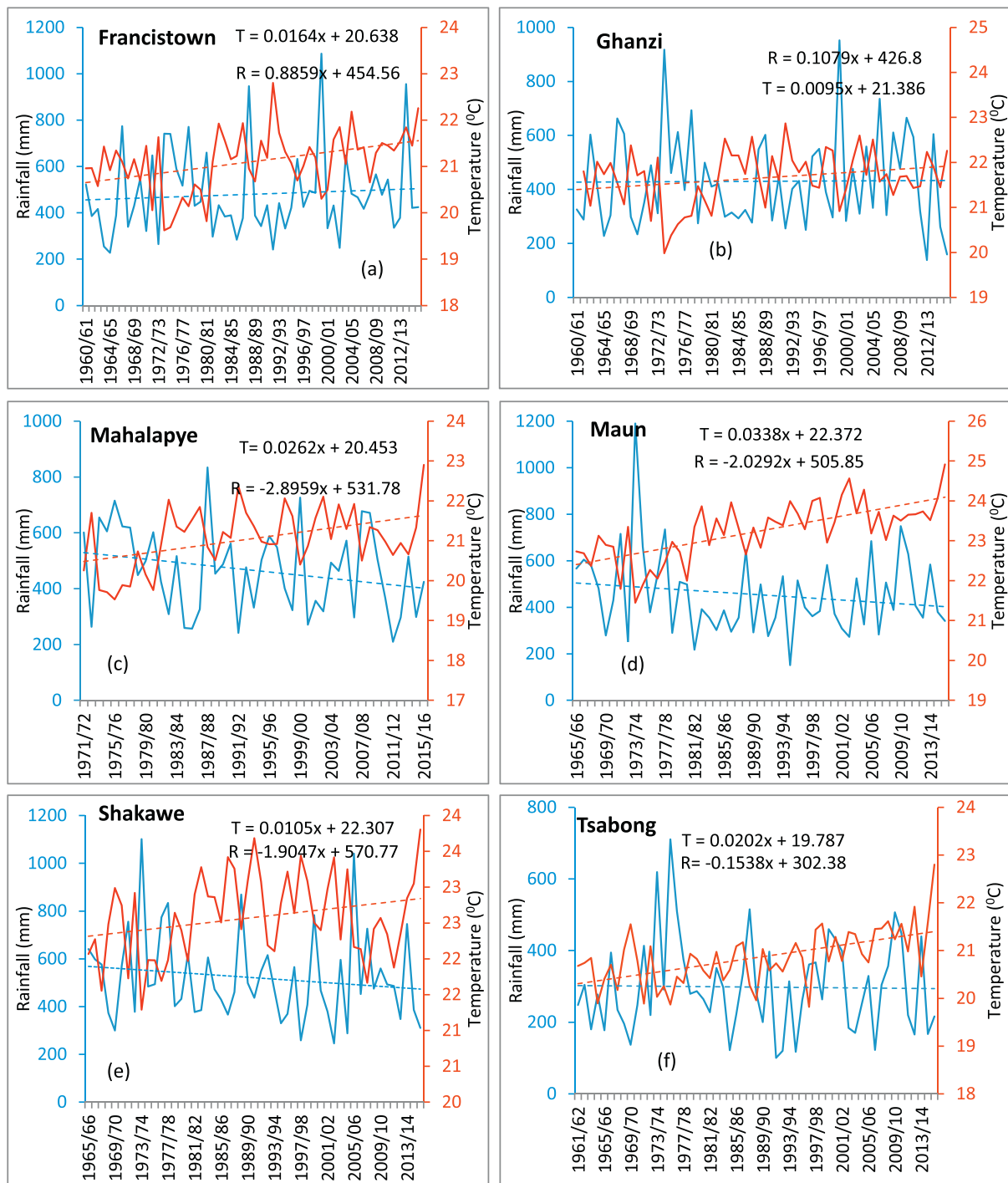
**Fig. 3.** Time series of rainfall (blue solid line) and temperature (red solid line) together with their linear trends (dotted lines) at selected synoptic stations from all regions across the study area. (For interpretation of the references to colour in this figure legend, the reader is referred to the web version of this article.)

transformation. The transformation gives SPEI time series with mean zero and standard deviation 1. The SPEI time series oscillate around the mean with positive values depicting wet spells while negative ones dry spells.

Computation of SPI follows the same procedure except steps (1) and (2) are omitted since SPI is only precipitation based. From step (3), instead of climatic water balance, precipitation values are directly used. For the case of SPI, rainfall time series were found to fit the generalized extreme value function (GEV) most of the time.

### 3.1.1. SPEI calculation steps

i. Determination of potential evapotranspiration (ET₀)

The Hargreaves equation used for obtaining ET$_0$ as presented in Allen et al. (1998) and Byakatonda et al. (2016) is given by;

$$ET_{0m} = 0.000938R_a(T_{mean} + 17.8)\sqrt{(T_{max} - T_{min})} \qquad (1)$$

where, $T_{mean}$ is the monthly mean temperature (°C), $T_{max}$ is the maximum air temperature (°C), $T_{min}$ is the minimum air temperature (°C) and $R_a$ is extraterrestrial radiation (MJ m$^{-2}$ d$^{-1}$).

The climatic water balance for any month m then becomes;

$$W_m = P_m - ET_{0m} \tag{2}$$

where $P_m$ is monthly rainfall totals.

ii. Aggregation of the climatic water balance $W_m$

The computed $W_m$ series are then aggregated at agreed timescales denoted by h-months. The aggregated $W_m$ series at h-months timescale for a given year i and month m can be presented as;

$$W_{i,m}^h = \begin{cases} \sum_{n=13-h+m}^{12} W_{i-1,n} + \sum_{n=1}^{m} W_{i,n} & \text{for } m < h \\ \sum_{n=m-h+1}^{12} W_{i,n} & \text{for } m \geq h \end{cases} \tag{3}$$

iii. Standardizing aggregated $W_m$ time series ($W_{i,\ m}^h$)

Since the $W_{i,\ m}^h$ series can possess both negative and positive values, 3-parameter distributions are used as candidate functions for fitting the series. L-moments for ordered $W_{i,\ m}^h$ series are used to select an appropriate distribution that fits the series. L-moments have also be found to be robust even for non uniformly distributed data which is common with small samples (Beguería et al., 2014; Hosking and Wallis, 2005). From the L-moment diagram, the GLO distribution was identified and is given by;

$$f(W_{i,m}^h) = \frac{\alpha^{-1} \exp[-(1-k)y]}{[1 + \exp(-y)]^2} \tag{4}$$

where y is also given by;

$$y = \begin{cases} -k^{-1} \log\left[1 - \frac{k(W_{i,m}^h - \xi)}{\alpha}\right], & k \neq 0 \\ \frac{(W_{i,m}^h - \xi)}{\alpha}, & k = 0 \end{cases} \tag{5}$$

The CDF of the GLO then follows as,

$$F(W_{i,m}^h) = \frac{1}{[1 + \exp(-y)]} \tag{6}$$

The parameters $\xi$, $\alpha$ and k represents the location, scale and shape of the distribution. Details of the GLO parameter estimation can be obtained in Byakatonda et al. (2016).

The CDF is then standardized into a normal variable D (SPEI) through an approximation suggested by Abramowitz and Stegun (1964) as follows;

$$D = Z - \frac{2.516 + 0.803Z + 0.0103Z^2}{1 + 1.433Z + 0.189Z^2 + 0.0013Z^3} \tag{7}$$

where,

$$Z = \sqrt{\left[\ln\left(\frac{1}{P^2}\right)\right]} \tag{8}$$

And P is the probability of exceeding given value of $W_{i,\ m}^h$.

A drought is registered when D values drop below zero and its duration is then taken as the time interval when D values are continuously negative. The magnitude of that drought episode is given by the summation of all D values during the duration of drought. The zero threshold is selected as the mean of the standardized D values and has been applied in other related studies as reported in Meza (2013) and Das et al. (2016).

### 3.1.2. SPI computation steps

The original formulation of SPI uses a 2-parameter gamma distribution (Guenang and Kamga, 2014; Lloyd-Hughes and Saunders, 2002). However, even though the gamma distribution is defined for zero precipitation, its corresponding probability density function defines the probability of obtaining zero precipitation as zero. This may not be true for dry locations with consecutive zero rainfall months. Hence the use of gamma distribution to generate SPI values in arid and semiarid climates could be challenging. Recently, the formulation of SPI has also been configured for Pearson Type III distribution since the pioneering work of Guttman (1999, 1998). The Pearson Type III distribution has also been used for SPI computations due in part to its superiority over the gamma distribution especially for the semiarid environments (Moalafhi et al., 2017). However, it is necessary to fit the data to the most suitable distribution to account for local attributes (Mishra and Singh, 2010). For this reason, the same procedure of PWMs and L-moments to identify the most appropriate distribution was applied in this study.

The procedure of aggregation as described in Eq. (3) was followed for rainfall series. From the L-moment diagram, a GEV distribution was identified to fit the aggregated rainfall series denoted by $P_{i,\ m}^h$. The GEV distribution is given by;

$$f(P_{i,m}^h) = \alpha^{-1} \exp[-(1-k)y - \exp(-y)] \tag{9}$$

where y is given by,

$$y = \begin{cases} -k^{-1} \ln\left[1 - \frac{k(P_{i,m}^h - \xi)}{\alpha}\right], & k \neq 0 \\ \frac{(P_{i,m}^h - \xi)}{\alpha}, & k = 0 \end{cases} \tag{10}$$

The cumulative density function of the GEV is given by;

$$F(P_{i,m}^h) = \exp[-\exp(-y)] \tag{11}$$

The formulations of parameters $\xi$, $\alpha$ and k are presented in Byakatonda et al. (2018). The approximation of the SPI utilizes the same procedure as explained in Eqs. (7) and (8).

### 3.2. Detection of monotonic trend in drought severity time series

This study investigated possible temporal trends in drought evolutions over the period of study. Trend detection can possibly be done using parametric or non parametric techniques. Parametric techniques require that the time series be normally distributed and independent which is rather a shortcoming while dealing with climatological data. Due to uncertainties in such datasets, this study uses two non parametric trend tests viz.: the Mann-Kendall statistic to test the direction of trend and Sen's slope estimator to determine the magnitude of the resulting trend.

### 3.2.1. Mann-Kendall trend statistic

The Mann-Kendall test statistic as suggested by Mann (1945) and Kendall M.G (1975) uses the S-statistic. The test depends on the rank of the values in the time series of D values representing SPI/SPEI. If the D series are represented by $d_1$, $d_2$, ....., $d_w$, each value is compared with the rest of the values in the time series. For any positive difference between values, the S-statistic is increased by 1 otherwise it is decreased by 1. The S-statistic remains constant while comparing equal data points. The S-statistic is given by;

$$S = \sum_{k}^{w-1} \sum_{m=k+1}^{w} Sgn(d_m - d_k) \tag{12}$$

where $m > k$, $d_m$ and $d_k$ are data points in the time series with w values while Sgn is given by;

$$Sgn(d_m - d_k) = \begin{cases} +1 & \text{if } (d_m - d_k) > 0 \\ 0 & \text{if } (d_m - d_k) = 0 \\ -1 & \text{if } (d_m - d_k) < 0 \end{cases} \tag{13}$$

Positive values of the S-statistic signify increasing trend (wet tendencies) while negative values decreasing trend (dry tendencies). To test the statistical significance of the detected trend, the Z-statistic (Z

stat) is normally used, The Z-statistic as applied in Yue et al. (2002), Gocic and Trajkovic (2013) and Golian et al. (2015) is given by;

$$
Z_{-stat} = \begin{cases} \dfrac{S-1}{\sqrt{\dfrac{w(w-1)(2w+5) - \sum_{m=1}^{r} t_m(t_m-1)(2t_m+5)}{18}}} & \text{if } S > 0 \\ 0 & \text{if } S = 0 \\ \dfrac{S+1}{\sqrt{\dfrac{w(w-1)(2w+5) - \sum_{m=1}^{r} t_m(t_m-1)(2t_m+5)}{18}}} & \text{if } S < 0 \end{cases}
$$

(14)

where r is the number of tied groups and $t_m$ number of ties of extent m. The null hypothesis being tested is that no trend exists in the drought severity time series. This null hypothesis is rejected if $|Z_{-stat}| > 1.96$ and significant trend exists. The threshold of 1.96 is obtained from the standard normal table at $\alpha = 0.05$ which is the level of significance used in this study. Positive trends signify wetting conditions while negative values drying tendencies.

### 3.2.2. Sen's slope estimator

The Mann-Kendall statistic is only able to identify the direction of the trend. To determine the magnitude of the trend, the non parametric Sen's slope estimator is applied. The Sen's slope as suggested by Sen (1968) and applied in Gocic and Trajkovic (2013) is given by

$$
Q_s = \frac{(d_m - d_k)}{m - k}
$$

(15)

The median of the slope of $Q_s$ series arranged in increasing order provides the Sen's slope estimate. The magnitude of the slope in this study is determined at a decadal scale and is denoted by D-units/10a.

### 3.2.3. Test for persistence in drought severity time series

The presence of serial correlation in the drought severity time series may increase the chances of rejecting the null hypothesis even when no trend exists (Gocic and Trajkovic, 2013; Partal and Kahya, 2006). To overcome this, pre-whitening of the time series is normally applied and this study utilized this technique prior to applying the Mann-Kendall test and Sen's slope estimator. The following steps were followed in order to remove any possible effect of serial correlation.

i. The lag-1 auto correlation coefficient $r_1$ was computed as applied in He et al. (2015) and Byakatonda et al. (2018c), it is given by;

$$
r_1 = \frac{\frac{1}{w-1} \sum_{i=1}^{w-1} (d_i - \overline{d})(d_{i+1} - \overline{d})}{\frac{1}{w} \sum_{i=1}^{w} (d_i - \overline{d})^2}
$$

(16)

where $\overline{d}$ is the mean of the drought severity time series.

ii. The confidence limits of $r_1$ at $\alpha = 0.05$ are computed as follows

$$
\frac{-1 - 1.96\sqrt{(w-2)}}{(w-1)} \le r_1 \le \frac{-1 + 1.96\sqrt{(w-2)}}{(w-1)}
$$

(17)

If the $r_1$ values fall within the limits in Eq. (17) above, then the SPI/SPEI series are assumed independent and the MK test is applied on the original series. If the $r_1$ falls outside the limits, the SPI/SPEI series were pre-whitened according to the procedure suggested by Partal and Kahya (2006) and applied in (He et al. (2015) as follows

$$
d_2 - r_1 d_1, \; d_3 - r_1 d_2, \; ....., d_w - r_1 d_{w-1}
$$

(18)

### 3.3. Association between SPI and SPEI

The relationship between the two drought indices is investigated through bivariate correlation analysis at each of the timescales used in this study. Due to uncertainties in climatological data and complex climate dynamics, the non parametric Spearman's rank correlation is applied to determine the degree of association. The Spearman's rank correlation $C_Y$ as suggested by Kottegoda and Rosso (2008) is used. The correlation coefficient is given by;

$$
C_Y = 1 - \frac{6 \sum_{i=1}^{w} Y^2}{w(w^2 - 1)}
$$

(19)

where Y is the difference in ranks between SPI and SPEI time series. The test for statistical significance is also computed from the Z-statistic given by;

$$
Z = C_Y \sqrt{\frac{(w-2)}{(1 - C_Y^2)}}
$$

(20)

The association is considered significant if the computed Z value in Eq. (20) is greater than a critical value obtained from a standard normal table at $\alpha = 0.05$.

## 4. Results

### 4.1. Drought temporal evolutions and characteristics

Drought temporal evolutions are presented in Figs. 4 and 5 at timescales of 3-, 6-, 12-, and 24-months. 1- and 18-months evolutions are not shown because they exhibit similar temporal behavior as those at 3- and 24-months timescale respectively. The evolutions presented here are from spatially representative stations located in all regions across the study area. The stations used are Francistown in the east, Ghanzi in the west, Maun in the north and Tsabong in the south. It is observed that both SPI and SPEI exhibit similar variations with notable differences in detection of onset and cessation of droughts. It is also observed that in some drought events, severity of drought differs across timescales. Both wet and dry spells are presented on the temporal evolutions but only drought events are reported in this paper. At lower timescales of 3- and 6-months, the temporal evolutions between wet and dry periods are of high frequency making it difficult to identify distinctive dry/wet spells during the period of analysis.

In the east at Francistown (Fig. 4), a drought event of 1960/ 61–1966/67 was well detected by both indices. However, SPI showed an earlier onset but ceded at the same time. SPI showed higher drought severity compared to SPEI. Both SPI and SPI were able to detect the next mild droughts of 1968/69–1969/70 and 1971/72–1973/74 with both showing equal severity but SPI recorded a higher duration. The longest drought on record in the eastern region was reported between 1980/81 and 1986/87. The same duration was recorded by both indices with SPI recording a higher severity in the final year of this drought episode. The second most damaging drought since 1960 on record was that between 1990/91 and 1993/94. This drought event was well detected by both indices in both duration and magnitude. The next drought event of 2001/02–2003/04 was equally reported by both indices with equal magnitude and duration. There was a mild drought of 2010/11–2012/13 in the eastern region which was only detected by SPI. The most recent hard biting drought of 2015/16 was only detected by SPEI with SPI completely missing it in the eastern region.

In the western region at Ghanzi (Fig. 4), the 1960/61–1967/68 drought reported in the east was also observed in the west but was much shorter and less in magnitude. The drought started in 1963/64 and ceded in 1965/66. The 1968/69–1970/71 drought recorded in the east was also detected in the west but was longer in duration terminating a year later. During this drought episode, SPI recorded higher drought severity than SPEI. The drought event of 1980/81–1986/87 was also observed in the west with SPI showing higher drought severity in the final year. The 1990/91–1993/94 drought was also recorded in the west but less severe than that reported in the east. 1998/99 was recorded as a drought year in the west by both indices. This event was never detected in the east. Another drought event of 2001/02–2003/04
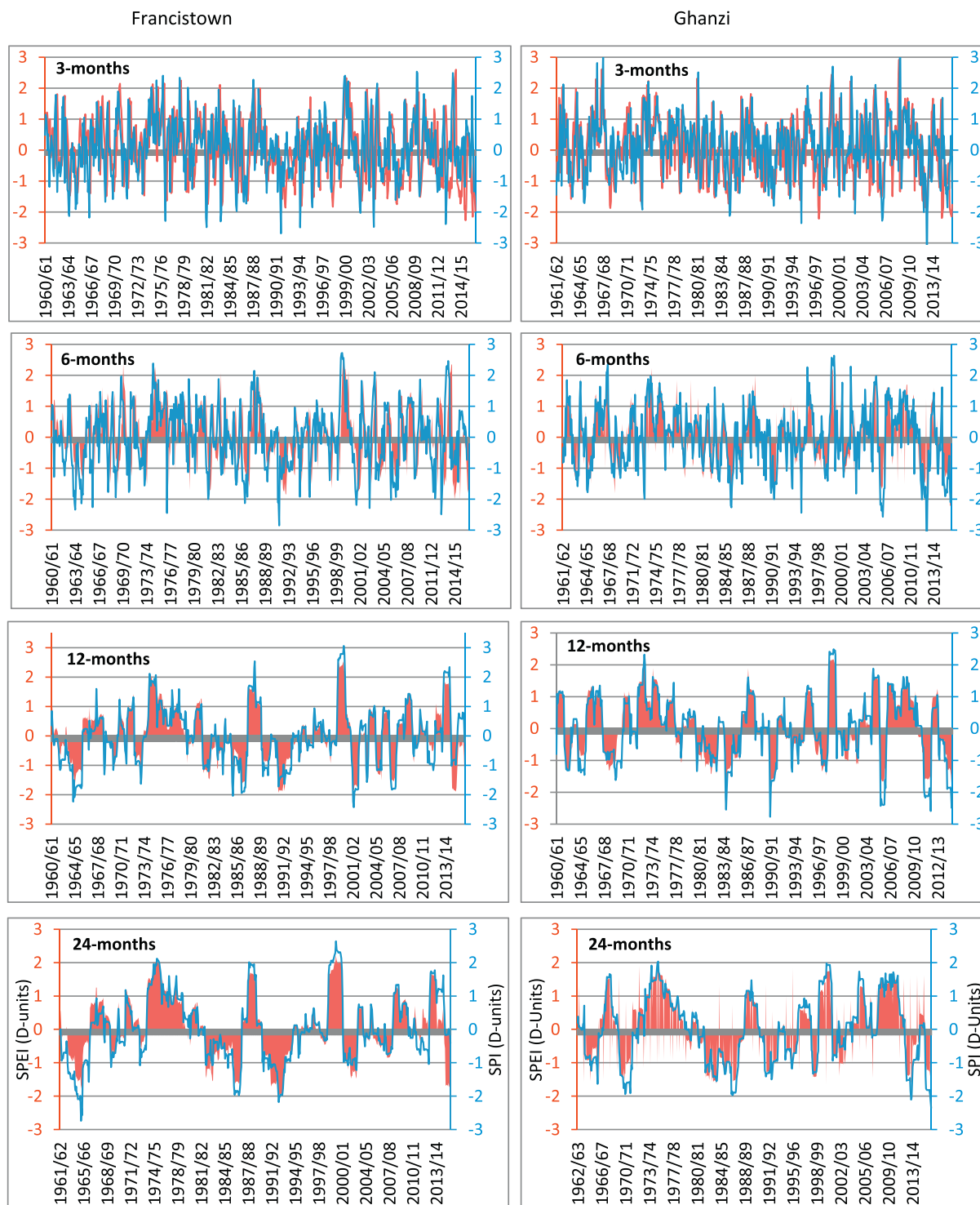
Francistown

Ghanzi



**Fig. 4.** Temporal evolution of SPI (Blue line) and SPEI (Red shaded area) for 3-, 6-, 12- and 24-months timescales recorded at Francistown in the east and Ghanzi in the west of the study area. SPEI/SPI = 0 is the threshold below which a drought event is registered. (For interpretation of the references to colour in this figure legend, the reader is referred to the web version of this article.)

was also detected with SPEI showing higher severity. The drought event of 2010/11–2012/13 which was only reported by SPI in the east was detected in this region by both indices although SPI recorded higher severity. The latest drought of 2015/16 was detected by both SPI and SPEI with the former registering higher drought severity.

In the north at Maun in Fig. 5, equally most drought events reported in the east and west were also detected. The 1968/69–1970/71 drought was registered with SPI showing higher severity but equal in duration.

The longest drought of the 1980s extended by a year ceding in 1987/88. The next drought on record started in 1990/91 but ceded earlier in 1992/93. This drought was briefly punctuated in 1993/94 resuming thereafter until 1998/99 although it was mild. The drought of 2001/02–2002/03 was detected by both indices only that SPI reported higher severities. In subsequent years, the northern region reported very mild droughts by both indices including the most recent of 2015/16.

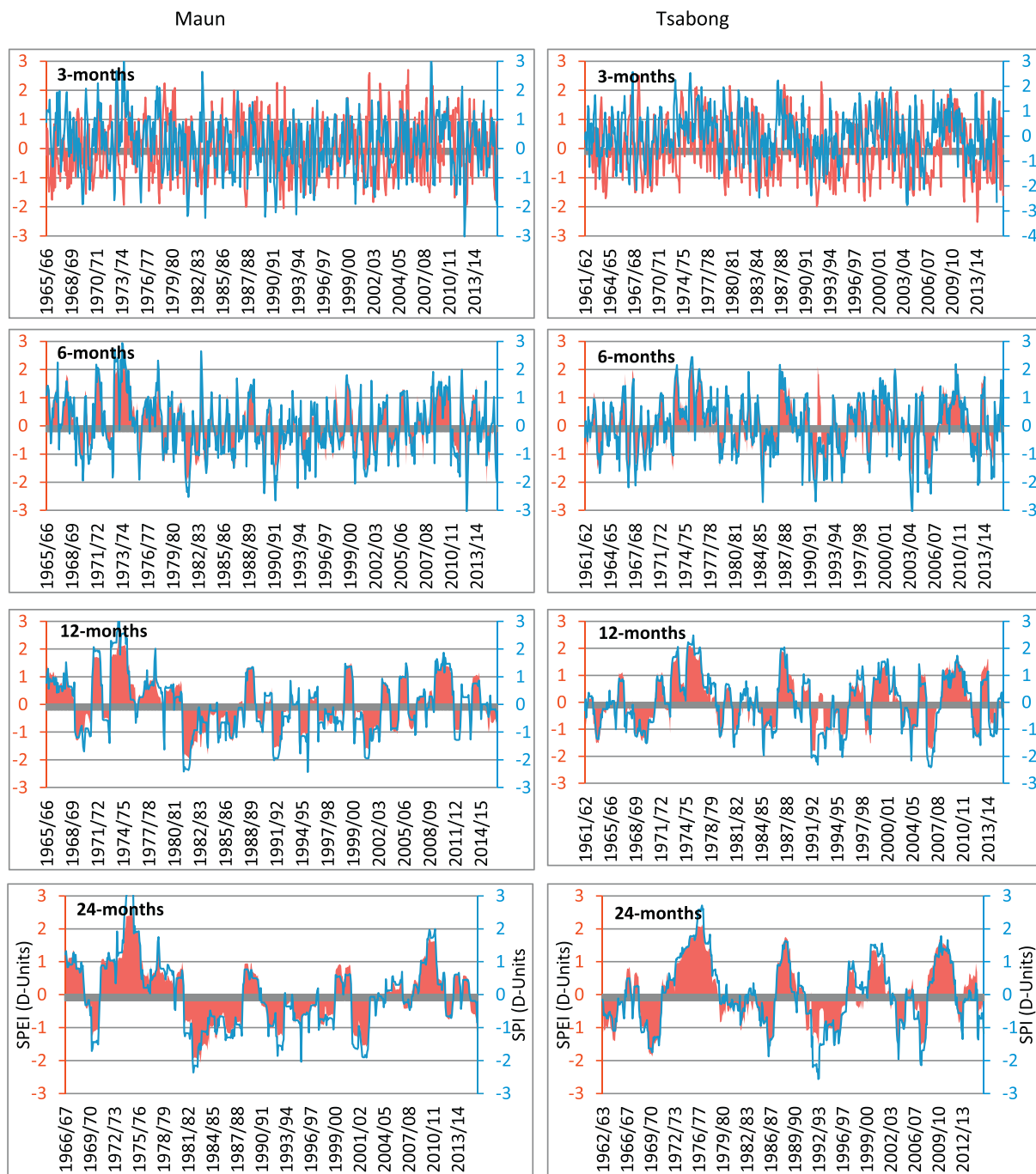In the south at Tsabong (Fig. 5), the 1960/61–1964/65 drought was

**Fig. 5.** Temporal evolution of SPI (Blue line) and SPEI (Red shaded area) for 3-, 6-, 12- and 24-months timescales recorded at Maun in the north and Tsabong in the south of the study area. SPEI/SPI = 0 is the threshold below which a drought event is registered. (For interpretation of the references to colour in this figure legend, the reader is referred to the web version of this article.)

detected by both indices. In contrast, SPEI recorded higher severity compared to SPI which had been registering higher values. The following drought event of 1967/68–1970/71 was longer by a year in comparison to other regions. Both indices registered the same level of drought severity for this episode. The period between 1978/79 and 1983/84 was characterized by mild droughts in this region. These mild droughts intensified into moderate droughts from 1984/85 ending in 1986/87. The next drought event in the region was from 1990/91 ceding in 1996/97. For this drought event, SPI registered higher severities in 1992/93. The 2001/02 droughts recorded in other regions came later in 2003/04 pausing the following year but again resuming in 2006/07 for a year later. The drought of 2012/13 was registered by

both indices not as the case in the eastern region. The 2015/16 drought event was also recorded as mild in the southern region by both indices. It is observed that drought events coincide across the study area with only differences in duration and magnitude in some cases. It is further observed that the indices were able to detect historical droughts disaster events on record. These historical events were reported to occur in 1961–1965, 1979–1987, 1991–1999, 2001–2005, 2009–2013 and 2014–2016 according to Botswana's recent disaster digest. It is also observed that SPI over estimates drought severity during the dry winter months across the study area at all the timescales. It was hence necessary to further investigate the years of maximum drought severity and months in which it occurred to observe any possible seasonality.

**Fig. 6.** Temporal evolution of droughts at 12-months timescale at all the 14 synoptic stations.

Also in an earlier study by the authors, it was discovered that climatic droughts take at least 6 months to propagate into hydrological systems (Byakatonda et al., 2018). This calls for further investigation of drought temporal evolution at 12-months timescale.

#### 4.1.1. Drought temporal evolution at 12-months timescale

Results for 12-months temporal evolutions at all the synoptic stations are presented in Fig. 6. For easier comparison, only temporal evolutions for the common period (2000–2016) are reported here. As mentioned in subsection 2.1, climate in Botswana is largely influenced by the shifting of the Inter Tropical Convergence Zone (ITCZ),

westerlies and easterlies. Also the Kalahari desert in the west, Okavango basin in the north and Limpopo basin in the southeast are other physical features that play a role in moderating the local climate. For this reason, the SPI and SPEI temporal evolutions are discussed regionally. From Fig. 6, in the east at Francistown, Mahalapye and Selibe-Phikwe, the 2001–2005 historical drought was detected but with an interruption in 2003–2004. The 2009–2013 historical drought was not that pronounced at Francistown as the case of Mahalapye and Selibe-Phikwe recorded by both indices. The most recent drought of 2014–2016 was also observed but more pronounced at Francistown and Selibe-Phikwe.

In the north at Maun, Kasane, Pandamatenga and Shakawe where

the influence of the ITCZ stands out, the 2001–2005 drought is well detected by the two drought indices. Just as the case in the east, it was also interrupted during 2003–2004. The 2009–2013 drought was delayed until 2010. This is not surprising since the region receives the highest rainfall across the study area. In the south at SSKA, the 2001–2005 drought was short only recorded in the first year and during the final year (2004–2005). At Jwaneng also in the south, this drought episode was not detected by both indices. The 2009–2013 drought was continuous overlapping into the 2014–2016 drought at SSKA. At Jwaneng the same drought was interrupted in 2013 before the 2014–2016 drought which was well detected at this location.In the central at Letlhakane and Sowa Pan, the 2001–2005 drought is well detected by the two indices at both stations. The 2009–2013 drought was short at these stations with Letlhakane registering it from 2010 to 2012 and Sowa Pan just one year from 2011 to 2012. The most recent drought of 2014–2016 was mainly detected by SPI though not pronounced. Implying that probably at these locations, the decrease in rainfall was the main driver of drought rather than temperature rise.

The west and southwest at Tshane, Tsabong and Ghanzi, the 2001–2005 drought was shortest at Ghanzi ending in 2003. The 2009–2013 drought was also short at all the stations in this region spanning a period between 2011 and 2013. The most recent drought of 2014–2016 was more pronounced at Ghanzi than any other location in this region. The temporal evolution of drought are observed to take similar patterns across the study area, this may be attributed to the flat topography of the study area that facilitates uniform atmospheric circulation.

### 4.1.2. Maximum drought severity and their period of occurrence

Results of the maximum drought severity are presented in Table 2 for both SPI and SPEI. These results revealed that drought severities that were registered during the historical period were either of moderate or severe categories. It is also observed that most of the severities

occurred during the summer months of October, November, December, January, February, March and April for both indices.

For SPI, severe droughts were recorded at Ghanzi, Jwaneng, Kasane, Mahalapye, Maun, Sowa Pan, Tsabong and Tshane. Ghanzi, located in the Kalahari desert, recorded the highest severity of −3.84 during winter season at 6-months timescale in July/2012. It is observed that winter months recorded maximum severity at timescales > 3-months. This could have been as a result of accumulating rainfall deficits over longer periods (whole season). The peak summer season of 2015/16 of December–January was observed to be a common period across the study area when maximum severity occurred.

For severity determined according to the SPEI procedure, all maximum drought severities on record were of moderate drought category. This could be in support of the fact that below normal rainfall does not necessarily translate into higher evaporation rates since it could occur during cold months. Generally SPEI is observed to register lower severities compared to SPI. Similarly as for the case of SPI, the summer of 2015/16 recorded the most maximum drought severities across the study area. Summer droughts are of great interest across the study area because majority of the rainfall is received during this season. Besides, the agricultural activities are also carried out during the summer season.

Since the summer of 2015/16 has been identified as a common period with maximum drought severity across the study area, this study went ahead to make spatial representation of drought severity for December-2015 at 12-months timescale. Results of spatial variability are presents in Fig. 7. From Fig. 7a, moderate droughts according to SPI are observed to increase from west and northwest to southern locations around Jwaneng. The east to northeast are observed not to be affected with near normal conditions largely registered. The southwest location at Tshane and Tsabong are also not severely affected during this period of high severity. Spatial variability of droughts as determined by SPEI is shown in Fig. 7b. It is observed that the pattern of areas under moderate

**Table 2**
Maximum drought severity and period it occurred during historical record.

| Station | SPI | | | | | | | | | | | |
|---|---|---|---|---|---|---|---|---|---|---|---|---|
| | 1-Month | | 3-Month | | 6-Month | | 12-Month | | 18-Month | | 24-Month | |
| | Dmax | Year/Month | Dmax | Year/Month | Dmax | Year/Month | Dmax | Year/Month | Dmax | Year/Month | Dmax | Year/Month |
| Francistown | −2.92 | 1965/Dec | −2.69 | 1990/Nov | −2.85 | 1990/Nov | −2.43 | 2002/Mar | −2.61 | 1964/Jul | −2.74 | 1964/Nov |
| Ghanzi | −3.11 | 1994/Dec | −3.76 | 2013/Apr | −3.84 | 2012/Jul | −2.77 | 1992/Feb | −2.59 | 2014/Jan | −2.35 | 2015/Dec |
| Jwaneng | −3.23 | 1993/Jan | −2.54 | 1994/Nov | −2.65 | 1994/Nov | −2.78 | 2015/Dec | −2.47 | 2016/Jun | −2.76 | 2015/Dec |
| Kasane | −2.70 | 1992/Feb | −2.40 | 2002/Dec | −2.37 | 1992/Feb | −2.43 | 2014/Jan | −3.01 | 2013/Jul | −2.40 | 2002/Dec |
| Letlhakane | −2.38 | 2015/Feb | −2.20 | 2013/Apr | −2.20 | 2012/Jul | −1.93 | 1999/Feb | −1.92 | 1998/Aug | −1.89 | 2015/Feb |
| Mahalapye | −3.27 | 2002/Nov | −2.40 | 2002/Jan | −2.62 | 2002/Mar | −2.70 | 2011/Oct | −2.39 | 2013/Apr | −2.54 | 1987/Feb |
| Maun | −2.38 | 1972/Nov | −3.02 | 2013/Apr | −3.05 | 2012/Jul | −2.44 | 1994/Dec | −2.43 | 1981/Sep | −2.36 | 1983/Mar |
| Pandamatenga | −2.13 | 2013/Mar | −2.57 | 2015/Dec | −2.56 | 2015/Dec | −1.97 | 2015/Jan | −1.82 | 2011/Nov | −2.19 | 2015/Jan |
| Selibe-Phikwe | −2.33 | 2015/Jan | −2.28 | 2000/Nov | −2.06 | 2007/Oct | −2.02 | 2001/Oct | −2.05 | 2013/Jun | −2.27 | 2012/Dec |
| Shakawe | −2.65 | 1995/Jan | −2.59 | 1972/Nov | −2.56 | 1972/Nov | −2.43 | 1995/Jan | −2.25 | 2001/Nov | −2.23 | 1999/Mar |
| SSKA | −2.06 | 1985/Nov | −2.51 | 2010/Nov | −2.40 | 2010/Nov | −2.66 | 2016/Jan | −2.56 | 2013/Mar | −2.48 | 2013/May |
| Sowa Pan | −3.06 | 2009/Dec | −1.99 | 2013/Apr | −2.08 | 2012/Jul | −2.13 | 1995/Feb | −1.73 | 1994/Jul | −1.93 | 2004/Jan |
| Tsabong | −2.41 | 1964/Jan | −2.76 | 2005/Jan | −3.17 | 2005/Feb | −2.41 | 2006/Aug | −2.40 | 1991/Sep | −2.56 | 1992/Dec |
| Tshane | −2.47 | 2007/Feb | −2.68 | 1990/Dec | −3.05 | 1992/Jan | −2.88 | 1992/Mar | −2.71 | 1965/Mar | −2.53 | 1964/Sep |
| **SPEI** | | | | | | | | | | | | |
| Francistown | −2.44 | 1986/Jun | −2.27 | 2014/Sep | −2.02 | 2014/Oct | −1.94 | 1992/Mar | −2.07 | 1991/Dec | −2.10 | 1993/Mar |
| Ghanzi | −2.51 | 1998/Jun | −2.22 | 1997/Jul | −2.22 | 2015/Nov | −1.82 | 2015/Dec | −2.04 | 2015/Dec | −1.76 | 2015/Dec |
| Jwaneng | −2.23 | 2016/Feb | −2.19 | 1997/Jun | −1.82 | 2015/Dec | −1.91 | 2015/Dec | −1.77 | 2016/Mar | −1.87 | 1999/Dec |
| Kasane | −2.51 | 2004/Jun | −2.05 | 1996/May | −2.14 | 2004/Nov | −2.18 | 2002/12 | −2.11 | 2002/Jun | −2.15 | 1986/Dec |
| Letlhakane | −2.40 | 2002/Apr | −2.39 | 2001/Jul | −2.14 | 2005/Sep | −2.05 | 1999/Feb | −1.97 | 1998/Aug | −1.94 | 1999/Mar |
| Mahalapye | −2.51 | 1993/Jun | −2.21 | 2002/Jan | −2.25 | 2002/Jan | −1.85 | 2011/Oct | −1.79 | 2001/Oct | −1.82 | 1989/Nov |
| Maun | −2.27 | 1998/Jun | −2.04 | 1991/Dec | −2.07 | 2014/Oct | −2.05 | 1981/Nov | −1.98 | 1992/May | −2.08 | 1984/Jan |
| Pandamatenga | −2.51 | 2005/Jun | −1.90 | 2015/Dec | −1.89 | 2015/Dec | −1.60 | 2014/Feb | 1.63 | 2011/Nov | −1.70 | 2011/Nov |
| Selibe-Phikwe | −2.20 | 2015/May | −1.93 | 2008/Sep | −1.72 | 2002/Mar | −1.66 | 2001/Oct | −1.99 | 2003/Feb | −1.85 | 2003/Mar |
| Shakawe | −2.41 | 2007/Sep | −2.28 | 2015/Dec | −2.29 | 2015/Dec | −2.04 | 1995/Jan | −1.80 | 1999/May | −1.91 | 1996/Jan |
| SSKA | −2.52 | 1998/Jun | −2.37 | 2006/Sep | −1.81 | 1992/May | −1.78 | 2016/Jan | −1.75 | 2013/Mar | −1.78 | 1992/Oct |
| Sowa Pan | −1.93 | 2002/Jul | −2.49 | 1997/Aug | −1.82 | 2004/Nov | −1.87 | 1995/Feb | −1.72 | 2003/Jun | −1.76 | 2002/Nov |
| Tsabong | −2.52 | 2013/Jun | −2.52 | 2012/Jul | −2.10 | 1992/Jun | −1.85 | 1992/Apr | −1.91 | 1970/Mar | −1.88 | 1970/Nov |
| Tshane | −2.43 | 1978/Aug | −2.01 | 1975/Sep | −1.95 | 1964/Apr | −2.00 | 1963/Sep | −2.16 | 1965/Feb | −2.06 | 1965/May |
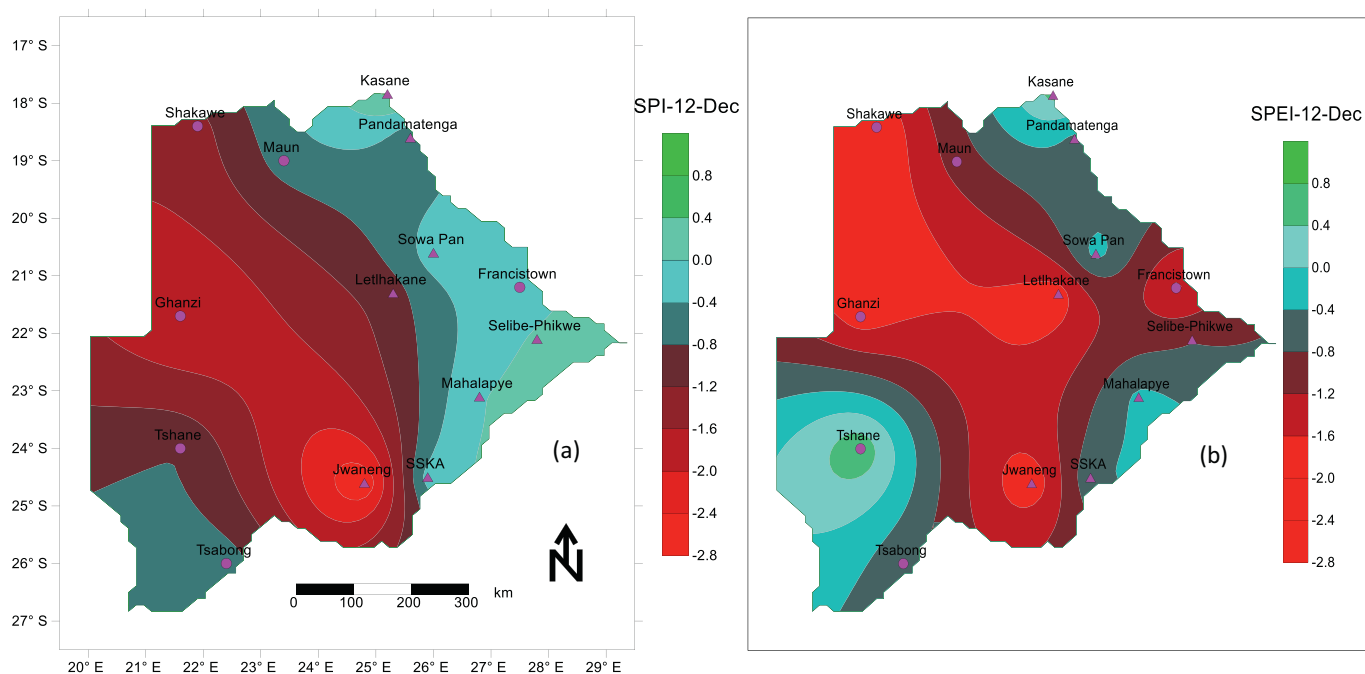
**Fig. 7.** Spatial distribution of drought severity evolutions in Dec-2015 (one of the driest year on record) (a) SPI-evolutions and (b) SPEI evolutions showing vulnerable areas under SPI/SPEI < 0.

drought are similar to those observed with SPI except that the eastern locations at Francistown and Selibe-Phikwe, which were not vulnerable under SPI, are now seen to be drier. The area under moderate drought vulnerability is seen to have increased while using SPEI for drought assessment. The area under drought resulting from SPI < 0 is measured to be 491,098 km$^2$ while that under SPEI < 0 is 555,428 km$^2$ translating into 92.5% of the country's total land area. This is rather a large discrepancy in the reporting of spatial coverage of droughts while using these drought indices. The drying gradient is still observed to take a northwest to south direction.

### 4.2. Trend analysis of drought severity time series

#### 4.2.1. Mann-Kendall (MK) trends in SPI time series for the entire period of 1960–2016

Results from this analysis are presented in Table 3. From these results, drought severity time series derived using SPI showed mostly negative trends (drying conditions) most of the time across the study area at all timescales used in this study. Trends are observed to be generally lower than those derived from SPEI series (SPEI series registered higher trends than SPI at the same station). These results are presented for 1-, 3-, 6-, 12-, 18- and 24-months timescale. At 1-month timescales all stations showed drying tendencies during the historical period except at Francistown. For the 1-month timescale, none of the trends recorded (positive or negative) were significant at 95% confidence interval. At 3-months timescale again only Francistown showed a positive trend (wetting conditions) with 93% of the stations showing drying trends. The positive trend could be attributed to the increasing trend in rainfall at Francistown reported in Fig. 3. The negative trend was only significant at Pandamatenga with a drying rate of −0.209 D-units/10a. At 6-months timescale, drying trends were observed at 71% of the stations but only significant at Pandamatenga with a drying rate of −0.246 D-units/10a. For the 12-months timescale, drying trends were observed at 79% of the stations. These trends were significant at Letlhakane and Pandamatenga with drying rates of −0.065 and −0.087 D-units/10a respectively. 18-months timescale trends showed that 86% of the stations recorded drying tendencies during the historical period. None of these trends were significant at 95%

confidence interval. Equally the 24-months timescale trends showed that 86% of the stations across the study area recorded drying tendencies. At this timescale however, significant trends were only observed at Kasane, Mahalapye, Pandamatenga, Shakawe and SSKA. The drying rates at these stations were −0.015, −0.009, −0.042, −0.007 and −0.024 D-units/10a respectively. Most stations exhibit negative trends (drying tendencies), this is in agreement with results in Fig. 3 which indicates that rainfall has decreased across all regions in Botswana except in the east at Francistown.

#### 4.2.2. Mann-Kendall (MK) trends in SPEI time series for the entire period of 1960–2016

Results from this analysis are also presented in Table 3. For 1-month SPEI trend analysis, records indicated drying conditions at 93% of the stations used in this study. Positive trends are only observed at Mahalapye though not significant. Drying trends were observed to be significant at Francistown, Ghanzi, Jwaneng, Kasane, Maun, Pandamatenga and Shakawe. The rates of drying at these stations were − 0.081, −0.06, −0.222, −0.147, −0.079, −0.257 and − 0.165 D-units/10a respectively. Interestingly, Francistown which showed a wetting tendency at this timescale with SPI series is now registering significantly drying trends. This is attributed to increase in evaporative demand resulting from temperature rise recorded over the same period at Francistown. This implies that in using only one drought index especially SPI, results must be interpreted with caution. At 3-months timescale all stations showed drying tendencies except at Maun. Significant drying trends are observed at Pandamatenga and Shakawe. The drying rates at these locations were − 0.206 and − 0.055 D-units/10a respectively. For the 6-months timescale, drying trends were also observed at 76% of the stations. These trends were significant at Jwaneng and Shakawe at a rate of − 0.108 and − 0.039 D-units/10a respectively. For the 12-months timescale series, drying tendencies are observed at 86% of the stations with significant trends at Jwaneng, Letlhakane, Mahalapye, Pandamatenga and Shakawe. The drying trends at these stations were −0.112, −0.098, −0.012, −0.075 and −2.495 D-units/10a respectively. For the 18-months SPEI series, drying conditions were also observed at 93% of the stations. The only significant drying trend was recorded at Mahalapye with a drying rate of −0.068

**Table 3**
Trend analysis tests results for Z-statistic and Sen's slope magnitude (1960–2016).

| Station | Test | SPI timescales (Months) | | | | | | SPEI timescales (Months) | | | | | |
|---|---|---|---|---|---|---|---|---|---|---|---|---|---|
| | | 1 | 3 | 6 | 12 | 18 | 24 | 1 | 3 | 6 | 12 | 18 | 24 |
| Francistown | Z-stat | 0.330 | 0.144 | 0.839 | 1.309 | 0.878 | 0.646 | −3.382* | −1.473 | −0.434 | −0.231 | −0.323 | −0.527 |
| | D-units/10a | 0.001 | 0.003 | 0.012 | 0.008 | 0.006 | 0.002 | −0.081 | −0.025 | −0.006 | −0.001 | −0.004 | −0.002 |
| Ghanzi | Z-stat | −0.655 | −0.730 | 0.216 | −0.092 | −0.334 | 0.235 | −2.435* | −1.339 | −1.264 | −0.811 | −0.226 | −0.738 |
| | D-units/10a | −0.006 | −0.012 | 0.003 | 0.000 | −0.002 | 0.001 | −0.060 | −0.023 | −0.022 | −0.003 | −0.001 | −0.007 |
| Jwaneng | Z-stat | −1.131 | −1.158 | −0.999 | −1.132 | −0.668 | −0.734 | −3.140* | −1.493 | −2.202* | −1.973* | −1.410 | −0.522 |
| | D-units/10a | −0.061 | −0.056 | −0.034 | −0.018 | −0.012 | −0.008 | −0.222 | −0.074 | −0.108 | −0.112 | −0.053 | −0.031 |
| Kasane | Z-stat | −0.594 | −0.796 | −0.851 | −0.853 | −0.536 | −2.110* | −2.720* | −0.537 | −0.743 | −0.432 | −0.193 | 0.096 |
| | D-units/10a | −0.009 | −0.028 | −0.030 | −0.009 | −0.008 | −0.015 | −0.147 | −0.025 | −0.033 | −0.017 | −0.004 | 0.002 |
| Letlhakane | Z-stat | −1.180 | −1.449 | −1.253 | −2.437* | −0.918 | −1.100 | −0.220 | −0.015 | 0.107 | −1.994* | −0.141 | −0.659 |
| | D-units/10a | −0.050 | −0.105 | −0.080 | −0.065 | −0.028 | −0.019 | −0.023 | −0.001 | 0.007 | −0.098 | −0.004 | −0.031 |
| Mahalapye | Z-stat | −1.799 | −1.602 | −1.586 | −2.012* | −0.886 | −2.328* | 0.486 | −2.029* | −1.592 | −1.946* | −4.070* | −0.251 |
| | D-units/10a | −0.045 | −0.039 | −0.029 | −0.012 | −0.008 | −0.009 | 0.016 | −0.059 | −0.026 | −0.012 | −0.068 | −0.006 |
| Maun | Z-stat | −0.967 | −1.335 | −1.042 | −1.430 | −0.766 | −1.068 | −2.780* | 1.576 | −1.322 | −1.001 | −0.819 | −0.949 |
| | D-units/10a | −0.012 | −0.025 | −0.018 | −0.008 | −0.006 | −0.002 | −0.079 | 0.040 | −0.021 | −0.006 | −0.009 | −0.003 |
| Pandamatenga | Z-stat | −1.722 | −2.440* | −3.197* | −3.271* | −1.286 | −2.153* | −1.999* | −2.159* | −2.165* | −2.464* | −1.105 | −0.790 |
| | D-units/10a | −0.137 | −0.209 | −0.246 | −0.087 | −0.050 | −0.042 | −0.257 | −0.206 | −0.161 | −0.075 | −0.039 | −0.029 |
| Selibe-Phikwe | Z-stat | −0.150 | −0.178 | 0.066 | 0.310 | 0.256 | −0.192 | −0.822 | 0.181 | 1.760 | 1.044 | 0.299 | 0.487 |
| | D-units/10a | −0.011 | −0.016 | 0.006 | 0.012 | 0.015 | −0.003 | −0.131 | 0.020 | 0.170 | 0.060 | 0.020 | 0.026 |
| Shakawe | Z-stat | −0.931 | −1.443 | −1.501 | −1.202 | −0.711 | −2.235* | −6.175* | −3.051* | −2.688* | −2.495* | −1.358 | −6.568* |
| | D-units/10a | −0.009 | −0.029 | −0.026 | −0.006 | −0.006 | −0.007 | −0.165 | −0.055 | −0.039 | −0.012 | −0.009 | −0.088 |
| SSKA | Z-stat | −1.247 | −0.919 | −0.903 | −1.657 | −1.698 | −2.899* | −0.412 | −1.016 | −0.513 | −0.919 | −1.324 | −2.143* |
| | D-units/10a | −0.049 | −0.036 | −0.026 | −0.020 | −0.027 | −0.024 | −0.024 | −0.044 | −0.015 | −0.010 | −0.019 | −0.019 |
| Sowa Pan | Z-stat | −0.574 | −0.229 | 0.248 | 0.214 | 0.271 | −0.314 | −0.209 | 0.273 | 0.516 | 0.590 | 0.323 | 0.034 |
| | D-units/10a | −0.022 | −0.015 | 0.013 | 0.004 | 0.006 | −0.004 | −0.018 | 0.017 | 0.032 | 0.009 | 0.007 | 0.000 |
| Tsabong | Z-stat | −0.663 | −0.593 | −0.691 | −0.166 | −0.444 | −0.511 | −1.109 | −0.857 | −0.621 | 0.007 | −0.204 | −0.240 |
| | D-units/10a | −0.010 | −0.010 | −0.009 | −0.001 | −0.003 | −0.002 | −0.027 | −0.015 | −0.008 | 0.000 | −0.001 | −0.001 |
| Tshane | Z-stat | −0.768 | −0.796 | −0.788 | −0.839 | −0.928 | −0.535 | −0.918 | −0.674 | −0.604 | −0.233 | −0.333 | −0.275 |
| | D-units/10a | −0.008 | −0.014 | −0.011 | −0.005 | −0.006 | −0.001 | −0.023 | −0.013 | −0.009 | −0.003 | −0.002 | −0.001 |

Z-stat = Mann-Kendall test statistic.
D-units/10a = Sen's Slope magnitude (magnitude of change per decade).
  * Significant at 5% level of significance.

D-units/10a. Similarly the 24-months SPEI trends showed drying trends at 93% of the stations used in this study. Shakawe and SSKA recorded significant drying trends at rates of −0.088 and −0.019 D-units/10a respectively. The higher trends that are recorded for SPEI compared to SPI further demonstrate the importance of evaporation in the computation of drought severity under global warming conditions.

### 4.2.3. Mann-Kendall (MK) trends in SPI and SPEI time series for the earlier period of 1960–1979

The year 1980/81 was reported earlier in studies by Parida and Moalafhi (2008) and Byakatonda et al. (2018c) to be a year of intervention in rainfall and temperature time series in Botswana. For this reason, it was necessary in this study to understand the trends prior to this year and compare them with the combined period. Trends in SPI and SPEI series were analyzed for a period 1960–1979. Only six stations of Francistown, Ghanzi, Maun, Shakawe, Tsabong and Tshane had records dating to 1960 and hence they were those considered in this analysis. Results from this analysis are presented in Table 4. At 1-month timescale, analysis of SPI time series showed positive trends though none was significant. These trends were observed at majority of the stations used in this analysis. At 3-months timescale, a significant positive trend was observed at Francistown. The wetting rate at this station was 0.162 D-units/10a. At 6-months timescale Francistown still showed a significant wetting trend at a rate of 0.152 D-units/10a. For the 12-months SPI trends, significant positive trends were observed at Francistown, Tsabong and Tshane. The wetting rates at these stations were 0.075, 0.061 and 0.054 D-units/10a respectively. For the 18-months SPI, a significant positive trend was only observed at Francistown with a wetting gradient of 0.074 D-units/10a. The 24-months SPI trends showed similar behaviour with those at 12-months timescale. Significant positive trends were also observed at Francistown, Tsabong and Tshane with wetting gradients of 0.047, 0.045 and 0.037 D-units/

10a respectively being registered.

The SPEI trends mostly remained positive just as was the case with SPI. At 1-month timescale, none of the positive trends were significant. For the 3-months SPEI trends, a positively significant trend was observed at Maun with a wetting rate of 0.435 D-units/10a. The 6-months SPEI series did not show any significant trend at the six stations under consideration. The 12-months SPEI trends showed significant positive trends at Francistown and Tshane at rates of 0.061 and 0.170 D-units/10a respectively. For the 18-months series, only Francistown showed a positive trend at a gradient of 0.204 D-units/10a. The 24-months SPEI recorded significant positive trends at Francistown and Shakawe at rates of 0.039 and 0.365 D-units/10a respectively.

Spatial distributions of SPI-12 and SPEI-12 trends for the entire period are presented in Fig. 8. The SPI-12 trends (Fig. 8a) shows that trends along the western axis in the environs of the Kalahari desert are not experiencing drying tendencies. Drying trends are observed in the south, central, northeast and partly in the north. The eastern locations are not showing any signs of drying trends. The drying gradient is observed to progress from southern locations to northeast. Spatial distribution of trends for SPEI-12 presented in Fig. 8b shows that locations with drying tendencies reported by SPI are still observed to be exhibiting drying trends even with SPEI. It is evident that, the area under drying trends has increased spreading to north-western locations. The area under significantly drying trends as observed under SPI is 38,855 km² whereas that recorded by SPEI is 139,316 km². The significantly dry area as reported by SPI increased by almost 4 times while using SPEI. The south-western and eastern regions are still showing no drying conditions. Two drying gradients are observed with SPEI. Both gradients originate from the south with one progressing to the northeast and the other to the northwest.

**Table 4**

Trend analysis tests results for *Z*-statistic and Sen's slope magnitude (1960–1979).

| Station | Test | SPI timescales (Months) | | | | | | SPEI timescales (Months) | | | | | |
|---|---|---|---|---|---|---|---|---|---|---|---|---|---|
| | | 1 | 3 | 6 | 12 | 18 | 24 | 1 | 3 | 6 | 12 | 18 | 24 |
| Francistown | Z-stat | 1.796 | 2.007* | 2.130* | 2.957* | 2.114* | 2.607* | −0.390 | 0.417 | 1.053 | 2.320* | 3.489* | 2.186* |
| | D-units/10a | 0.165 | 0.162 | 0.152 | 0.075 | 0.074 | 0.047 | −0.044 | 0.033 | 0.070 | 0.061 | 0.204 | 0.039 |
| Ghanzi | Z-stat | 1.085 | 1.028 | 1.801 | 1.559 | 0.458 | 0.793 | 0.517 | 0.236 | 1.004 | 1.165 | 0.403 | 1.678 |
| | D-units/10a | 0.094 | 0.086 | 0.125 | 0.043 | 0.017 | 0.013 | 0.067 | 0.021 | 0.091 | 0.029 | 0.012 | 0.092 |
| Maun | Z-stat | −0.407 | −0.664 | −0.611 | 0.027 | −0.407 | −0.802 | −1.205 | 2.478* | −0.682 | 0.745 | 0.026 | −0.008 |
| | D-units/10a | −0.023 | −0.091 | −0.068 | 0.000 | −0.019 | −0.011 | −0.223 | 0.435 | −0.070 | 0.032 | 0.004 | 0.000 |
| Shakawe | Z-stat | 0.037 | −0.076 | −0.080 | 0.599 | 0.112 | 0.957 | 1.213 | 0.516 | 0.755 | 1.491 | 0.933 | 4.286* |
| | D-units/10a | −0.004 | −0.006 | −0.008 | 0.017 | 0.005 | 0.018 | 0.198 | 0.051 | 0.074 | 0.041 | 0.042 | 0.365 |
| Tsabong | Z-stat | 1.686 | 1.005 | 1.741 | 2.195* | 0.593 | 2.985* | 1.422 | 0.403 | 1.417 | 1.171 | −0.002 | 1.423 |
| | D-units/10a | 0.158 | 0.088 | 0.100 | 0.061 | 0.020 | 0.045 | 0.171 | 0.037 | 0.086 | 0.031 | 0.000 | 0.026 |
| Tshane | Z-stat | 1.019 | 1.098 | 1.913 | 2.052* | 0.893 | 2.081* | 0.979 | 0.499 | 1.434 | 2.271* | 0.593 | 1.778 |
| | D-units/10a | 0.083 | 0.091 | 0.144 | 0.054 | 0.032 | 0.037 | 0.130 | 0.050 | 0.115 | 0.170 | 0.021 | 0.029 |

Z-stat = Mann-Kendall test statistic.

D-units/10a = Sen's Slope magnitude (magnitude of change per decade).

\* Significant at 5% level of significance.

### 4.3. Association between SPI and SPEI

The Spearman rank correlation was used to study the degree of association between SPI and SPEI. Results from this analysis are presented in Fig. 9. During the analysis of both SPI and SPEI, correlations are observed to be lower at 1-month timescale increasing at higher timescales. This implies that rainfall is not the main driver of drought at lower timescales of 1 and 3-months. At most locations, the association increases steadily until 12-months timescale. Beyond 12-months the trend declines or sometimes remains constant at longer timescales with exceptional cases recorded at Jwaneng and Tshane all located in the southwest at the fringes of the Kalahari desert. At 12-months timescale which depicts seasonal variations, the highest correlation indicates that rainfall deficit is the dominant factor driving drought. The analysis show that SPI accounts for > 50% variations in SPEI across the study area. A median correlation plot was introduced to provide an overall trend of the degree of association between the two indices. This plot shows that the degree of association reaches its peak at 12-months timescale. The highest association recorded at this timescale was 96%.

From these observations, SPI can ably represent SPEI at 12-months timescale for those stations showing a high degree of association between the two indices. The 12-months could be a point of convergence since it is an accumulation of a complete meteorological year considering all seasons. It accounts for all deficits and possible surpluses that could have occurred during the year.

## 5. Discussion

### 5.1. Drought temporal evolutions and characteristics

This study analyzed the spatial and temporal drought evolutions across Botswana using SPI and SPEI during the period of 1960–2016. This is the first kind of study in this region using two drought indices. Both drought indices have demonstrated their ability to detect historical drought events of 1961–1965, 1981–1987, 1991–1999, 2001–2005, 2009–2013 and 2014–2016 as reported by Statistics Botswana (2016). The same events have been reported to occur on the African continent by Masih et al. (2014). These events were visible in
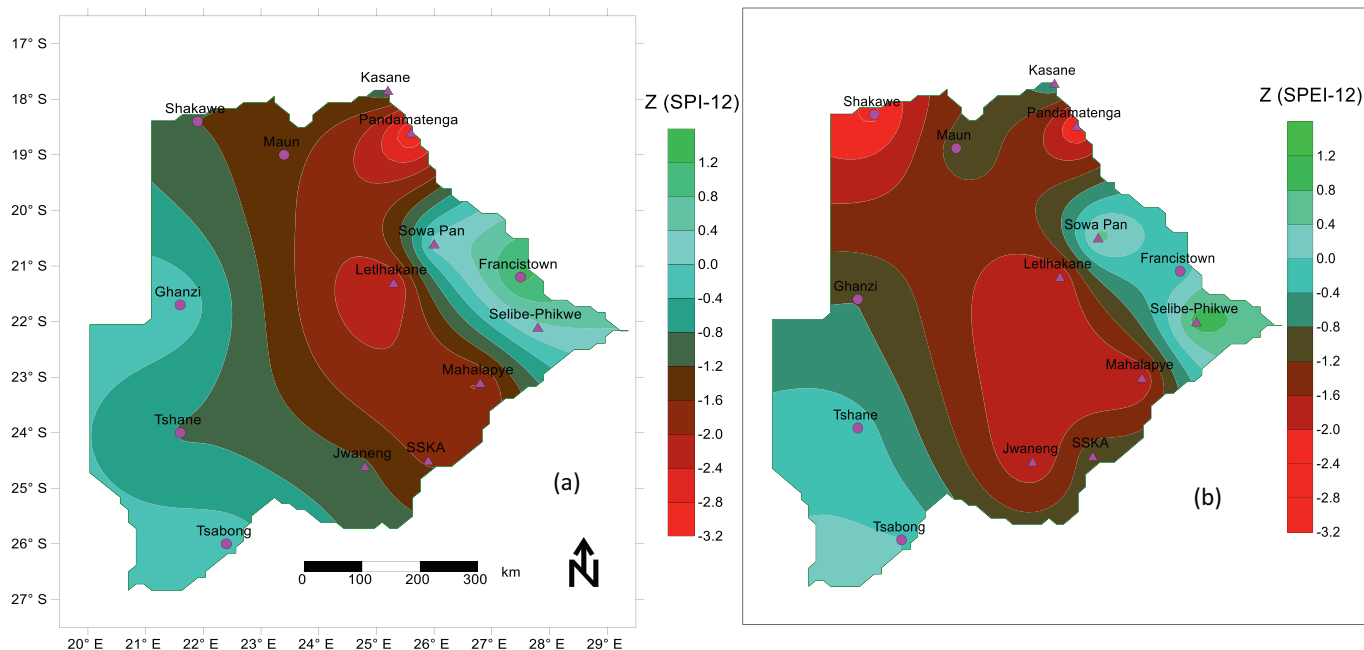


**Fig. 8.** Spatial distribution of Mann-Kendal trends at 12-months timescale (a) SPI-12 trends (b) SPEI-12 trends.
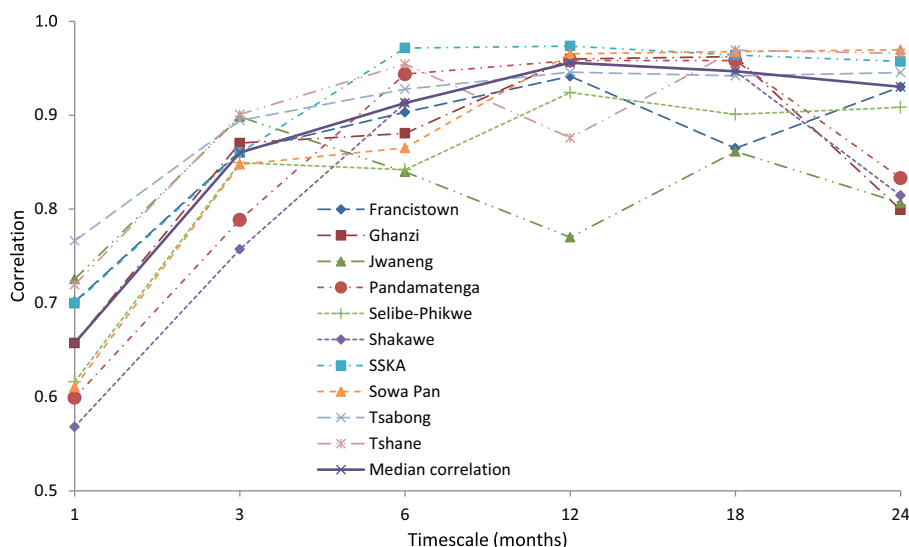
**Fig. 9.** Spearman rank correlation coefficients between SPI and SPEI for different study stations including median plot (solid line) across timescales.

evolutions at longer timescales since at shorter timescales the frequency between wet and dry spells is high to enable identification of drought impacts on hydrological systems. This corroborates findings from earlier studies of temporal evolution of droughts by Vicente-Serrano and López-Moreno (2005) and Homdee et al. (2016). Both indices recorded similar patterns however there were some notable differences in temporal evolutions. In cases where these differences occurred, SPI overestimated drought severity especially during the dry winter months. During the winter season, rainfall is largely suppressed with a number of years recording zero precipitation in consecutive months. Since only rainfall is used in the computation of SPI, it is not able to provide a realistic estimate of drought severity given that potential evapotranspiration ($ET_0$) rates are at their minimum during the same period. This could imply SPEI provides more reliable estimates since it takes care of both rainfall and evaporation. This finding is in agreement with those from studies conducted by Beguería et al. (2014) and Homdee et al. (2016) who reported poor performance of SPI in arid and semiarid climates. There is resounding evidence of global temperature rise especially during the 21st century (Cook et al., 2014; Dai, 2013; IPCC, 2012). It has also been projected that drought severity will follow suit. This study however does not show evidence of higher drought severity as a result of inclusion of $ET_0$ through the application of SPEI. A number of studies have pointed out that $ET_0$ is not only a function of temperature but also relative humidity, wind speed and solar radiation (Roderick et al., 2007; Vicente-Serrano et al., 2014). For this reason, a rise in temperature coupled with decreased wind speed may still not translate into high drought severity (Vicente-Serrano et al., 2015). Hence results from this study needs to be interpreted with caution since there is no long term time series of other variables other than temperature to enable their inclusion in computation of $ET_0$. Interestingly, the onset and cessation of historical drought events have been well represented by both indices. Devastating droughts of 1991/92 and 2015/16 recorded over southern Africa have been ably captured by both indices across the study area. This was evidenced with majority of maximum drought severities occurring in the summer of 2015/16. Many of these drought events also coincided with El Niño years of 1963/64, 1965/66, 1979/80, 1982/83, 1987/88, 1991/92, 2002/03, 2009/10, 2014/15 and 2015/16. It has been reported in earlier studies by Nicholson et al. (2001) and Byakatonda et al. (2018c) that rainfall across Botswana is suppressed during El Niño events. This could also point to the fact that El Niño has an influence on droughts. Spatial distribution of summer droughts showed that SPI underestimated drought vulnerable areas. The eastern locations were reported by SPI as

not showing signs of drying. The same locations are now shown to be vulnerable under SPEI. Nevertheless both indices indicate the southern region and the northwest to be highly vulnerable to summer droughts. This could be attributed to the fact that these locations are neighbouring the Kalahari desert. The vulnerability may also be associated with global trends of increasing aridity (Dai, 2013; Huang et al., 2016).

### 5.2. Trend analysis of drought severity

High spatial and temporal variability in rainfall and temperature time series have been reported in this study through presentations in Table 1, Figs. 2 and 3. This variability in climatic variables will ultimately lead to variant drought behaviours with time (Liu et al., 2016). This requires careful selection of a drought index that is sensitive to this variability in rainfall and temperature (Liu et al., 2016; Vicente-Serrano et al., 2010). This study therefore applied two multiscalar drought indices to evaluate the most suitable index that could represent these variations in climatic variables. From Figs. 2 and 3, it is observed that temperature has been on the increase across the study area during the period of analysis. At the same time rainfall has decreased during the same period in all regions except the east at Francistown and west at Ghanzi. SPI generally registered weaker trends compared to SPEI. This is in contrast to what Liu et al. (2016) reported for the semiarid Loess Plateau region of China. This discrepancy could be attributed to the flat topography of our study area that facilitates uniform atmospheric circulation. Further still the Loess Plateau's climate is heavily influenced by the Monsoon which could alter other climatic characteristics. The importance of inclusion of temperature and rainfall in determining drought severity was highlighted at Francistown. All trends reported by SPI were positive (wetting trends). These positive trends resulted because there was a reported increase in rainfall at that station. However, trends determined using SPEI at the same station were all negative (drying trends). This was also possible because there was a reported increase in temperature during the same period. This is another demonstration that the use of SPI in dry climates may give misleading results since in these locations temperature rise is evident (Dai, 2013; Huang et al., 2016; Modarres and da Silva, 2007). Pandamatenga in the northeast and Shakawe in the northwest are found to exhibit the most significant drying trends across the study area moreover in the most recent study by Byakatonda et al. (2018b), these locations were identified to be suitable for rainfed agriculture. This increase in drying trends may impede agricultural activities in these locations.

This study confirms that the period prior to 1980 was cooler and a

wet. During this period all significant trends were positive for both SPI and SPEI series. It was also evident that more severe droughts occurred after this suspected change year. This could support the assertion by Stocker et al. (2013) and Cook et al. (2014) that global warming has intensified during the 21st century. This calls for institutional changes that will combat the effects of climate variability and change. Spatial distribution of trends further shows that SPI underestimates the area susceptible to drying tendencies. This is a further demonstration that indices that incorporate more than one climatic variable are more suitable for detecting droughts than those using a single climatic variable such as SPI especially in arid and semiarid climates.

### 5.3. Association between SPI and SPEI

Results from this analysis reveal that at majority of the stations SPI accounted for > 50% of variations in SPEI. This is a clear manifestation that indeed rainfall deficiency is a dominant driver of drought. These findings are in agreement with those from studies by Masud et al. (2015) and Homdee et al. (2016) who reported high association between SPI and SPEI drought severity time series. The highest association at 12-months timescale signifies that accumulated rainfall deficits over 12-months is the main driver of drought. At this timescale where the degree of association is nearly perfect, SPI which is less data demanding may be used to represent SPEI. This is only possible at those specific stations where the degree of association is nearly 100%. However with drought severity showing higher spatial extent with SPEI and with the projected global warming trends, it is increasingly becoming necessary to use indices that incorporate temperature in describing drought characteristics.

### 6. Conclusion

This study characterized droughts at timescales of 1-, 3-, 6-, 12-, 18- and 24-months using two multiscalar drought indices for a period from 1960 to 2016. The monotonic trends in these drought characteristics were also investigated using the Mann-Kendall $Z$-statistic and Sen's slope estimator. The degree of association was determined in order to examine the extent to which one drought index can substitute the other. This is the first comprehensive study across Botswana that incorporates two drought indices to characterize and detect long term changes in drought severity. Based on the results and discussions, the following key points are put forward;

1. Both SPI and SPEI were able to detect historical drought events of 1961/62–1965/66, 1980/81–1986/87, 1991/92, 2001/02–2005/06, 2009/10–2012/13 and 2014/15–2015/16. Most of these events occurred during El Niño years hence the influence of ENSO on drought evolutions may not be ruled out. The evolutions were characterized with low frequency and longer duration at higher timescales of 12-, 18- and 24-months. Even though both indices were able to detect the historical events, SPI overestimated drought severity during the dry winter months. SPEI showed its superiority over SPI by exhibiting higher spatial coverage of drought vulnerability.

2. The period before 1980 showed significant wetting trends with both SPI and SPEI at Francistown and Tshane. However significantly drying trends were observed for the entire period (1960–2016) for both indices. Pandamatenga and Shakawe both agricultural areas recorded the most significantly drying trends during the period of analysis. The importance of temperature was demonstrated at Francistown where wetting trends were registered with SPI and drying trends with SPEI at all the timescales.

3. Rainfall deficiency was still found to be the dominant factor in drought occurrence with SPI accounting for > 50% in SPEI variations. The strongest degree of association of 96% was recorded at 12-months timescale. However, it is observed that other climatic

factors such as evaporation cannot be ignored in quantifying drought severity. This is as a result of ongoing global warming tendencies whose impacts are projected to even be higher in semi-arid locations.

The SPEI has been identified to be more robust in drought monitoring across Botswana. This information could go a long way in facilitating climate variability mitigation strategies in semiarid areas. It is further hoped that these efforts will increase resilience of local populations towards projected climate shocks if they can be assimilated into relevant decision making processes of climate variability adaptation strategies.

### Acknowledgment

### References

Abramowitz, M., Stegun, I.A., 1964. Handbook of Mathematical Functions: With Formulas, Graphs, and Mathematical Tables. Courier Corporation.

Alexandersson, H., 1986. A homogeneity test applied to precipitation data. J. Climatol. 6, 661–675.

Allen, R.G., Pereira, L.S., Raes, D., Smith, M., 1998. FAO irrigation and drainage paper no. 56. Rome Food Agric. Organ. United Nations 56, 97–156.

Batisani, N., 2011. The spatio-temporal-severity dynamics of drought in Botswana. J. Environ. Prot. (Irvine,. Calif) 2, 803.

Batisani, N., Yarnal, B., 2010. Rainfall variability and trends in semi-arid Botswana: implications for climate change adaptation policy. Appl. Geogr. 30, 483–489.

Beguería, S., Vicente-Serrano, S.M., Reig, F., Latorre, B., 2014. Standardized precipitation evapotranspiration index (SPEI) revisited: parameter fitting, evapotranspiration models, tools, datasets and drought monitoring. Int. J. Climatol. 34, 3001–3023. https://doi.org/10.1002/joc.3887.

Byakatonda, J., Parida, B.P., Kenabatho, P.K., 2018. Relating the dynamics of climatological and hydrological droughts in semiarid Botswana. Phys. Chem. Earth 1–13. https://doi.org/10.1016/j.pce.2018.02.004.

Byakatonda, J., Parida, B.P., Kenabatho, P.K., Moalafhi, D.B., 2016. Modeling dryness severity using artificial neural network at the Okavango Delta, Botswana. Glob. Nest J. 18, 463–481.

Byakatonda, J., Parida, B.P., Kenabatho, P.K., Moalafhi, D.B., 2018b. Prediction of onset and cessation of austral summer rainfall and dry spell frequency analysis in semiarid Botswana. Theor. Appl. Climatol. 1–17. https://doi.org/10.1007/s00704-017-2358-4.

Byakatonda, J., Parida, B.P., Kenabatho, P.K., Moalafhi, D.B., 2018c. Influence of climate variability and length of rainy season on crop yields in semiarid Botswana. Agric. For. Meteorol. 248. https://doi.org/10.1016/j.agrformet.2017.09.016.

Byakatonda, J., Parida, B.P., Kenabatho, P.K., Moalafhi, D.B., 2018d. Analysis of rainfall and temperature time series to detect long-term climatic trends and variability over semi-arid Botswana. J. Earth Syst. Sci. 127, 25. https://doi.org/10.1007/s12040-018-0926-3.

Cook, B.I., Smerdon, J.E., Seager, R., Coats, S., 2014. Global warming and 21st century drying. Clim. Dyn. 43. https://doi.org/10.1007/s00382-014-2075-y.

Dai, A., 2011. Drought under global warming: a review. Wiley Interdiscip. Rev. Clim. Chang. 2, 45–65. https://doi.org/10.1002/wcc.81.

Dai, A., 2013. Increasing drought under global warming in observations and models. Nat. Clim. Chang. 3, 52–58.

Das, P.K., Dutta, D., Sharma, J.R., Dadhwal, V.K., 2016. Trends and behaviour of meteorological drought (1901–2008) over Indian region using standardized precipitation–evapotranspiration index. Int. J. Climatol. 36, 909–916.

Edossa, D.C., Woyessa, Y.E., Welderufael, W.A., 2014. Analysis of droughts in the central region of South Africa and their association with SST anomalies. Int. J. Atmos. Sci. 2014.

GOB-MMEWR, 2006. National Water Mater Plan Review. Vol. 3 Gaborone, Botswana.

Gocic, M., Trajkovic, S., 2013. Analysis of changes in meteorological variables using Mann-Kendall and Sen's slope estimator statistical tests in Serbia. Glob. Planet. Change 100, 172–182.

Golian, S., Mazdiyasni, O., Aghakouchak, A., 2015. Trends in meteorological and agricultural droughts in Iran. Theor. Appl. Climatol. 119, 679–688.

Guenang, G.M., Kamga, F.M., 2014. Computation of the Standardized Precipitation Index (SPI) and its use to assess drought occurrences in Cameroon over recent decades. J. Appl. Meteorol. Climatol. 53, 2310–2324.

Guttman, N.B., 1998. Comparing the palmer drought index and the standardized precipitation index. JAWRA J. Am. Water Resour. Assoc. 34, 113–121.

Guttman, N.B., 1999. Accepting the standardized precipitation index: a calculation algorithm. JAWRA J. Am. Water Resour. Assoc. 35, 311–322.

Hänsel, S., Medeiros, D.M., Matschullat, J., Petta, R.A., de Mendonça Silva, I., 2016. Assessing homogeneity and climate variability of temperature and precipitation series in the capitals of north-eastern Brazil. Front. Earth Sci. 4, 1–21. https://doi.org/10.3389/feart.2016.00029.

Hayes, M., Svoboda, M., Wall, N., Widhalm, M., 2011. The Lincoln declaration on drought indices: universal meteorological drought index recommended. Bull. Am. Meteorol. Soc. 92, 485–488.

He, Y., Ye, J., Yang, X., 2015. Analysis of the spatio-temporal patterns of dry and wet conditions in the Huai River basin using the standardized precipitation index. Atmos. Res. 166, 120–128.

Heim Jr., R.R., 2002. A review of twentieth-century drought indices used in the United States. Bull. Am. Meteorol. Soc. 83, 1149–1165.

Homdee, T., Pongput, K., Kanae, S., 2016. A comparative performance analysis of three standardized climatic drought indices in the Chi River basin, Thailand. Agric. Nat. Resour. 50, 211–219.

Hosking, J.R.M., Wallis, J.R., 2005. Regional Frequency Analysis: An Approach Based on L-Moments. Cambridge University Press.

Huang, J., Ji, M., Xie, Y., Wang, S., He, Y., Ran, J., 2016. Global semi-arid climate change over last 60 years. Clim. Dyn. 46, 1131–1150.

IPCC, 2012. Managing the Risks of Extreme Events and Disasters to Advance Climate Change Adaption. Cambridge University Press.

Kenabatho, P.K., Parida, B.P., Moalafhi, D.B., 2012. The value of large-scale climate variables in climate change assessment: the case of Botswana's rainfall. Phys. Chem. Earth 50–52, 64–71. https://doi.org/10.1016/j.pce.2012.08.006.

Kendall, M.G., 1975. Rank Correlation Methods, 4th ed. London.

Kottegoda, N.T., Rosso, R., 2008. Applied Statistics for Civil and Environmental Engineers. Blackwell, Malden, MA.

Kumar, R., Musuuza, J.L., Van Loon, A.F., Teuling, A.J., Barthel, R., Ten Broek, J., Mai, J., Samaniego, L., Attinger, S., 2016. Multiscale evaluation of the Standardized Precipitation Index as a groundwater drought indicator. Hydrol. Earth Syst. Sci. 20, 1117.

Liu, Z., Wang, Y., Shao, M., Jia, X., Li, X., 2016. Spatiotemporal analysis of multiscalar drought characteristics across the loess plateau of China. J. Hydrol. 534, 281–299.

Lloyd-Hughes, B., Saunders, M.A., 2002. A drought climatology for Europe. Int. J. Climatol. 22, 1571–1592.

Mann, H.B., 1945. Nonparametric tests against trend. Econ. J. Econom. Soc. 245–259.

Masih, I., Maskey, S., Mussá, F.E.F., Trambauer, P., 2014. A review of droughts on the African continent: a geospatial and long-term perspective. Hydrol. Earth Syst. Sci. 18, 3635.

Masud, M.B., Khaliq, M.N., Wheater, H.S., 2015. Analysis of meteorological droughts for the Saskatchewan River basin using univariate and bivariate approaches. J. Hydrol. 522, 452–466.

McEvoy, D.J., Huntington, J.L., Abatzoglou, J.T., Edwards, L.M., 2012. An evaluation of multiscalar drought indices in Nevada and eastern California. Earth Interact. 16, 1–18.

McKee, T.B., Doesken, N.J., Kleist, J., et al., 1993. The relationship of drought frequency and duration to time scales. In: Proceedings of the 8th Conference on Applied Climatology, pp. 179–183.

Meza, F.J., 2013. Recent trends and ENSO influence on droughts in northern Chile: an application of the standardized precipitation evapotranspiration index. Weather Clim. Extrem. 1, 51–58.

Mishra, A.K., Singh, V.P., 2010. A review of drought concepts. J. Hydrol. 391, 202–216.

Mishra, A.K., Sivakumar, B., Singh, V.P., 2015. Drought processes, modeling, and mitigation. J. Hydrol. 526, 1–2.

Moalafhi, D.B., Sharma, A., Evans, J.P., 2017. Reconstructing hydro-climatological data using dynamical downscaling of reanalysis products in data-sparse regions–application to the Limpopo catchment in southern Africa. J. Hydrol. Reg. Stud. 12, 378–395.

Modarres, R., da Silva, V., De, P.R., 2007. Rainfall trends in arid and semi-arid regions of Iran. J. Arid Environ. 70, 344–355.

Nalbantis, I., Tsakiris, G., 2009. Assessment of hydrological drought revisited. Water Resour. Manag. 23, 881–897.

Nicholson, S.E., Leposo, D., Grist, J., 2001. The relationship between El Niño and drought over Botswana. J. Clim. 14, 323–335.

Oguntunde, P.G., Lischeid, G., Abiodun, B.J., Dietrich, O., 2014. Analysis of spatial and temporal patterns in onset, cessation and length of growing season in Nigeria. Agric.

For. Meteorol. 194, 77–87. https://doi.org/10.1016/j.agrformet.2014.03.017.

PaiMazumder, D., Sushama, L., Laprise, R., Khaliq, M.N., Sauchyn, D., 2013. Canadian RCM projected changes to short-and long-term drought characteristics over the Canadian prairies. Int. J. Climatol. 33, 1409–1423.

Palmer, W.C., 1965. Meteorological Drought. US Department of Commerce, Weather Bureau Washington, DC.

Parida, B.P., Moalafhi, D.B., 2008. Regional rainfall frequency analysis for Botswana using L-moments and radial basis function network. Phys. Chem. Earth 33, 614–620. https://doi.org/10.1016/j.pce.2008.06.011.

Partal, T., Kahya, E., 2006. Trend analysis in Turkish precipitation data. Hydrol. Process. 20, 2011–2026. https://doi.org/10.1002/hyp.5993.

Pettit, A.N., 1979. Anon-parametric approach to the change-point detection. Appl. Stat. 28, 126–135.

Roderick, M.L., Rotstayn, L.D., Farquhar, G.D., Hobbins, M.T., 2007. On the attribution of changing pan evaporation. Geophys. Res. Lett. 34.

Sen, P.K., 1968. Estimates of the regression coefficient based on Kendall's tau. J. Am. Stat. Assoc. 63, 1379–1389.

Sheffield, J., Wood, E.F., Roderick, M.L., 2012. Little change in global drought over the past 60 years. Nature 491, 435–438.

Shukla, S., Steinemann, A.C., Lettenmaier, D.P., 2011. Drought monitoring for Washington state: indicators and applications. J. Hydrometeorol. 12, 66–83.

Stagge, J.H., Tallaksen, L.M., Xu, C.Y., Van Lanen, H.A.J., 2014. Standardized precipitation-evapotranspiration index (SPEI): Sensitivity to potential evapotranspiration model and parameters. In: Proc. FRIEND-Water, pp. 367–373.

Statistics Botswana, 2009. Botswana Water Statistics. Vol. 3 Gaborone, Botswana.

Statistics Botswana, 2016. Botswana Environment Statistics: Natural Disasters Digest 2015. Gaborone, Botswana.

Stocker, T.F., Qin, D., Plattner, G.K., Tignor, M., Allen, S.K., Boschung, J., Nauels, A., Xia, Y., Bex, V., Midgley, P.M., 2013. Climate change 2013: the physical science basis. In: Intergovernmental Panel on Climate Change, Working Group I Contribution to the IPCC Fifth Assessment Report (AR5). New York.

Svoboda, M., Fuchs, B., et al., 2016. Handbook of Drought Indicators and Indices.

Usman, M.T., Reason, C.J.C., 2004. Dry spell frequencies and their variability over southern Africa. Clim. Res. 26, 199–211. https://doi.org/10.3354/cr026199.

Van Loon, A.F., 2013. On the Propagation of Drought: How Climate and Catchment Characteristics Influence Hydrological Drought Development and Recovery. Wageningen University.

Van Loon, A.F., Laaha, G., 2015. Hydrological drought severity explained by climate and catchment characteristics. J. Hydrol. 526, 3–14.

Vicente-Serrano, S.M., Begueria, S., López-Moreno, J.I., 2010. A multiscalar drought index sensitive to global warming: the standardized precipitation evapotranspiration index. J. Clim. 23, 1696–1718.

Vicente-Serrano, S.M., Begueria, S., Lorenzo-Lacruz, J., Camarero, J.J., López-Moreno, J.I., Azorin-Molina, C., Revuelto, J., Morán-Tejeda, E., Sanchez-Lorenzo, A., 2012. Performance of drought indices for ecological, agricultural, and hydrological applications. Earth Interact. 16, 1–27.

Vicente-Serrano, S.M., Chura, O., López-Moreno, J.I., Azorin-Molina, C., Sanchez-Lorenzo, A., Aguilar, E., Moran-Tejeda, E., Trujillo, F., Martínez, R., Nieto, J.J., 2015. Spatio-temporal variability of droughts in Bolivia: 1955-2012. Int. J. Climatol. 35. https://doi.org/10.1002/joc.4190.

Vicente-Serrano, S.M., López-Moreno, J.I., 2005. Hydrological response to different time scales of climatological drought: an evaluation of the standardized precipitation index in a mountainous Mediterranean basin. Hydrol. Earth Syst. Sci. Discuss. 9, 523–533.

Vicente-Serrano, S.M., Lopez-Moreno, J.-I., Beguería, S., Lorenzo-Lacruz, J., Sanchez-Lorenzo, A., Garcia-Ruiz, J.M., Azorin-Molina, C., Morán-Tejeda, E., Revuelto, J., Trigo, R., et al., 2014. Evidence of increasing drought severity caused by temperature rise in southern Europe. Environ. Res. Lett. 9, 44001.

Wang, K., Dickinson, R.E., Liang, S., 2012. Global atmospheric evaporative demand over land from 1973 to 2008. J. Clim. 25, 8353–8361.

Wijngaard, J.B., Klein Tank, A.M.G., Können, G.P., 2003. Homogeneity of 20th century European daily temperature and precipitation series. Int. J. Climatol. 23, 679–692.

Wilhite, D.A., 2000. Drought as a Natural Hazard: Concepts and Definitions.

Yue, S., Pilon, P., Phinney, B., Cavadias, G., 2002. The influence of autocorrelation on the ability to detect trend in hydrological series. Hydrol. Process. 16, 1807–1829. https://doi.org/10.1002/hyp.1095.